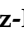


Article

Pseudo-nitzschia Blooms in a Coastal Upwelling System: Remote Sensing Detection, Toxicity and Environmental Variables

Jesús M. Torres Palenzuela ^{1,*}, Luis González Vilas ¹, Francisco M. Bellas ¹, Elina Garet ², África González-Fernández ²  and Evangelos Spyarakos ³ 

¹ Remote Sensing and GIS Laboratory, Department of Applied Physics, Sciences Faculty, University of Vigo, Campus Lagoas Marcosende, 36310 Vigo, Spain; luisgv@uvigo.es (L.G.V.); curro@uvigo.es (F.M.B.)

² Immunology Area, Biomedical Research Center (CINBIO) and Institute of Biomedical Research of Vigo (IBIV), University of Vigo, Campus Lagoas Marcosende, 36310 Vigo, Spain; melgaret@uvigo.es (E.G.); africa@uvigo.es (Á.G.-F.)

³ Biological and Environmental Sciences, School of Natural Sciences, University of Stirling, Stirling FK9 4LA, UK; evangelos.spyrakos@stir.ac.uk

* Correspondence: jesu@uvigo.es; Tel.: +34-986-812631

Received: 17 July 2019; Accepted: 16 September 2019; Published: 19 September 2019



Abstract: The NW coast of the Iberian Peninsula is dominated by extensive shellfish farming, which places this region as a world leader in mussel production. Harmful algal blooms in the area frequent lead to lengthy harvesting closures threatening food security. This study developed a framework for the detection of *Pseudo-nitzschia* blooms in the Galician *rias* from satellite data (MERIS full-resolution images) and identified key variables that affect their abundance and toxicity. Two events of toxin-containing *Pseudo-nitzschia* were detected (up to 2.5 $\mu\text{g L}^{-1}$ pDA) in the area. This study suggests that even moderate densities of *Pseudo-nitzschia* in this area might indicate high toxin content. Empirical models for particulate domoic acid (pDA) were developed based on MERIS FR data. The resulting remote-sensing model, including MERIS bands centered around 510, 560, and 620 nm explain 73% of the pDA variance ($R^2 = 0.73$, $p < 0.001$). The results show that higher salinity values and lower $\text{Si}(\text{OH})_4/\text{N}$ ratios favour higher *Pseudo-nitzschia* spp. abundances. High pDA values seem to be associated with relatively high PO_4^{3-} , low NO_3^- concentrations, and low $\text{Si}(\text{OH})_4/\text{N}$. While MERIS FR data and regionally specific algorithms can be useful for detecting *Pseudo-nitzschia* blooms, nutrient relationships are crucial for predicting the toxicity of these blooms.

Keywords: *Pseudo-nitzschia*; domoic acid; MERIS algorithms; upwelling; Galician *rias*

1. Introduction

Pseudo-nitzschia Peragallo is a chain-forming diatom genus that is widespread in all oceans of the world [1]. A number of these diatom species of this genus are known producers of a neurotoxic amino acid, domoic acid (DA), which when accumulated via trophic transfer in the food-web can have deleterious (amnesic shellfish poisoning, ASP) and even fatal effects to several marine organisms and less frequently to humans [2–4]. *Pseudo-nitzschia* is the only diatom genus among 27 dinoflagellates and 1 raphidophyte species that is listed as responsible for harmful algal events in upwelling regions [5]. *Pseudo-nitzschia* is generally common in upwelling systems e.g., in California Current System [6–10], in Iberian System [11–14], and Benguela upwelling system [15–17].

Understanding the relationships between the abundance of these diatoms, DA, and the characteristics of the environment will provide valuable information on the variable(s) that might determine their growth, distribution, and DA production. Several authors [18–24] have related these

blooms with changes in nutrient availability, and therefore with upwelling events and eutrophication. On the west coast of USA, an area where *Pseudo-nitzschia* is a common harmful bloom former, DA outbreaks that are caused by *P. australis* have been associated with upwelling events and increased but in declining phase nutrients [25,26]. Other authors have also found a relationship between high *Pseudo-nitzschia* spp. cell abundance and low-nutrient conditions [27–29]. Several laboratory experiments [30–35] have addressed the silicic acid and/or phosphorus, iron, copper limitations as significant factors for the toxin production of *Pseudo-nitzschia* species. The relationship between DA production and the nutritional status appears to be complex in natural populations, since they are often composed of several species [36,37], in fact some authors have not found obvious environmental triggers of DA production [16]. However, it seems that the silicic acid supply [7,9,20,24,28,38,39] plays an important role. More specifically for *P. australis*, Anderson [9] suggested that weight ratio values of $\text{Si(OH)}_4:\text{NO}_3^-$ below 2 are found to be linked to DA production from this species. Recently, Trick et al. [40] showed that iron and copper limitations, and not macronutrient stress, are more essential for the DA production in natural populations in the Pacific North-West.

In addition to nutrient availability, salinity has also been reported as an important factor that affects *Pseudo-nitzschia* abundance and/or DA production, mainly in estuarine systems [23,24,26,29,41]. Regarding temperature, although *Pseudo-nitzschia* species are observed in a wide range of temperatures, some authors have identified the optimal ranges for specific species [23,39]. Moreover, in a recent work, [42] report that warming could lead to an increase of abundance and toxicity of *Pseudo-nitzschia* spp. blooms in California coastal waters. Other environmental factors identified as affecting to *Pseudo-nitzschia* spp. distribution and bloom dynamics are light intensity [23,39], photoperiod [38], and factors controlling nutrient availability, such as river flow [29], rainfall [23,38], or upwelling [10,13,14].

Harmful algal events that were attributed to the genus *Pseudo-nitzschia* are considered as a reoccurring phenomenon along the northern boundary of the Iberian–Canary current upwelling system. These blooms have become a focal point of numerous studies since the first time that they were recorded in the autumn of 1994 [43] and they are occasionally associated with sporadic DA production, which occurs primarily towards the latter stages of bloom development [26]. Although several species of *Pseudo-nitzschia* have been recorded in the Galician coastal embayments referred to as *rias* (NW Spain), only *P. australis* has been shown to produce DA in the region [44]. Toxicogenic events due to blooms of *P. australis* in this area have been recorded before DSP (Diarrhetic Shellfish Poisoning) events [45] in thermohaline stratified water masses.

There is considerable interest in the study of *Pseudo-nitzschia* and the detection of DA in the Galician *rias* due to the economic and social importance of the extensive mussel culture in this region and human health concerns [46,47]. As part of a routine monitoring programme, the Technological Institute for the Control of the Marine Environment of Galicia (INTECMAR) has organized sampling on a weekly basis in the Galician *rias*, where, among other water parameters, *Pseudo-nitzschia* spp. abundance and biotoxins in mussels and other molluscs are recorded. DA detection in this area has been mainly studied on shellfish extracts [48,49] and on *Pseudo-nitzschia* cultures [44,50]. However, very limited information is available on the particulate DA concentrations (pDA) in seawater.

Chlorophyll *a* (*chl**a*) concentration can be used as a phytoplankton biomass indicator, since it is common to almost taxonomic groups [51]. Thus, *chl**a* maps that were derived from passive ocean colour sensors could be useful for identifying and monitoring high biomass blooms, although they do not provide information regarding species or toxicity [52]. In Galicia, MERIS imagery has already proven to be an effective tool to map the spatial and temporal distribution of high biomass algae events during an upwelling cycle [53]. MERIS provides images with a 300 m spatial resolution in nadir (Full Resolution –FR mode) and fifteen bands from visible to near infrared to support the monitoring of coastal zones [54]. Although MERIS is not operative since 2012, Sentinel-3 OLCI provides continuity to the MERIS dataset since 2016, providing the same spatial resolution (300 m), but with more spectral bands (21 instead of 15) ranging from 400 nm to 1020 nm [55].

The aim of this study is two-fold. Firstly, it attempts to develop a framework for the detection of potentially toxic *Pseudo-nitzschia* spp. blooms that are based on satellite data. Secondly, it aims to identify key variables affecting the formation and toxicity of *Pseudo-nitzschia* spp. blooms during different seasonally and meteorologically defined conditions, typical in upwelling systems.

2. Materials and Methods

2.1. Study Area

The Galician *rias* are V-shaped coastal formations along the northwest part of the Iberian Peninsula. The *rias* Baixas are the four southern *rias*, from north to south: Muros, Arousa, Pontevedra, and Vigo, all being oriented in a SW-NE direction (Figure 1a). This study focuses on two *rias* (Pontevedra and Vigo, Figure 1b), each being connected to the open sea through two entrances, to the north and south of the islands located at the external part of each *ria*. Rivers located in the innermost part of the *rias* provide the primary freshwater input [56].

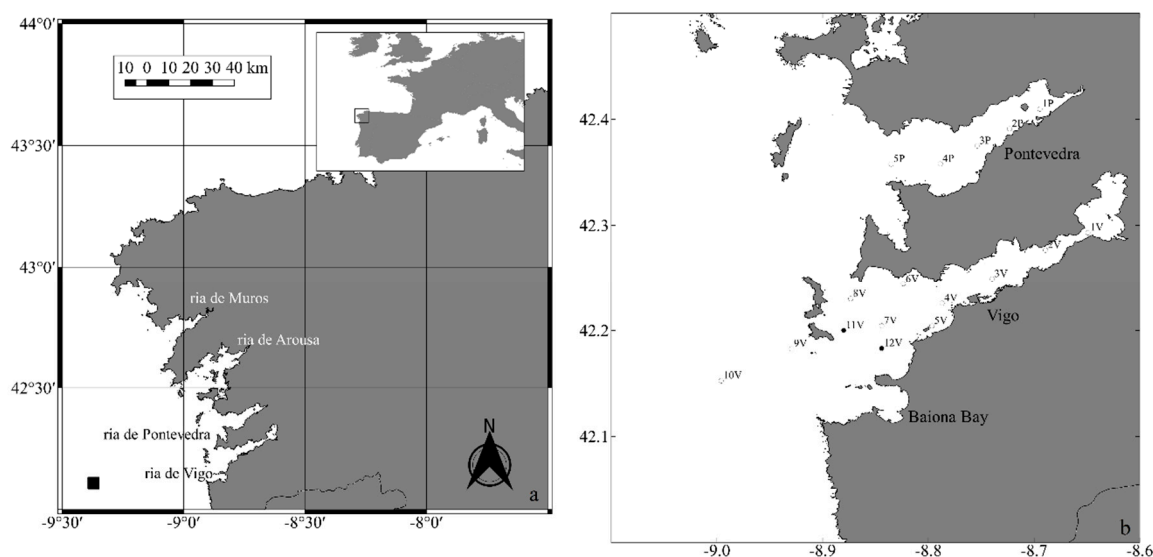


Figure 1. (a) Map of the Galician coast. From north to south the *rias* Baixas: Muros y Noya, Arousa, Pontevedra and Vigo. The location of the Seawatch buoy station off Cabo Silleiro is shown by a black rectangle. (b) Map of Ria de Vigo and Ria de Pontevedra showing the locations of the sampling stations.

2.2. Sampling Regime and In Situ Measurements

The samples were collected in two Galician *rias* during seven field trips (Table 1, Figure 1b) over a three-year period (2007–2009). Three periods were selected reflecting the different seasons of the campaigns and the meteorological conditions of the study area (Figure 2). Period 1 (spring downwelling) corresponds to spring downwelling conditions. The campaigns that were carried out on period 2 (summer) were characterised mainly by upwelling conditions or relaxation after strong upwelling favourable winds. This is typical of the summer upwelling-downwelling cycle in the area. The last period (period 3, autumn downwelling) includes campaigns in autumn and it is characterised by strong downwelling-favourable winds. These periods are considered as recurrent events in the coastal upwelling system of the Galician *rias* and they have been associated with harmful events due to diatoms or/and dinoflagellates in previous studies (review by [57]).

Ten fixed stations were visited five times (25 July 2007; 19 October 2007; 9 July 2008; 22 July 2008; 14 July 2009) in the Ria de Vigo, while using a sampling transect extended from the open sea toward the inner part of the *ria*. Two additional sampling stations, shown in Figure 1b as closed circles, were sampled on 14 July 2009. The depth of the stations ranged from 5 m inside the *ria* to 100 m in the outer part. Moreover, a five station transect was sampled twice (27 May and 7 July) in Ria de

Pontevedra during 2009 (Table 1), while using a transect extended from the middle part of the *ria* to the innermost part.

Chl a fluorescence profiles were monitored by a Turner designs CYCLOPS-7 submersible fluorometer. A portable meter provided the profiles of water temperature, pH, and dissolved oxygen (DO) (HI 9829, Hanna instruments). A Seabird Model 25 CTD was used to collect vertical profiles of temperature, salinity, fluorescence, and depth of water column at each site. Triplicate water samples from surface to 3 m were collected at each station from an integrated polycarbonate tubular water sampler (3524 cm 3) for further analysis, which is described below. The depth of the euphotic zone was established with a Secchi disk (Secchi disk depth or Zsd), while using measurements recorded by the same observer and taken from the sunny side of the boat.

Table 1. Summary of the field campaign, showing date, *ria*, number of sampling stations (#stations), period (between 1 and 3), sky conditions and the acquisition time and mean view zenith angle from west for the MERIS FR images used in this study. The three periods were: 1: Spring downwelling favourable winds; 2: summer upwelling-downwelling cycle and 3: autumn strong downwelling favourable winds.

Date	<i>ria</i>	#stations	Period	Sky Conditions	Acquisition Time (UTC)	View Zenith Angle (°)
25 July 2007	Vigo	10	2	clear	11:11	15.3
19 October 2007	Vigo	10	3	clear	11:08	12.6
9 July 2008	Vigo	10	2	clear	11:10	13.0
22 July 2008	Vigo	10	2	clear	11:02	11.7
27 May 2009	Pontevedra	5	1	clear	10:51	20.7
7 July 2009	Pontevedra	5	2	cloudy	10:58	15.7
14 July 2009	Vigo	12	2	partly cloudy	10:42	20.7

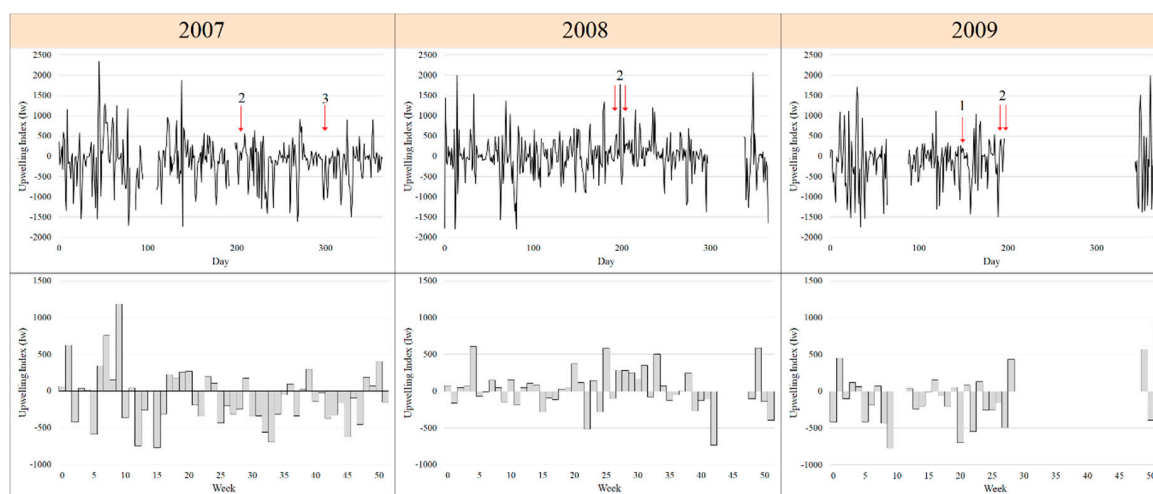


Figure 2. Daily and weekly upwelling index off the *rias Baixas* for the years 2007–2009. The I_w in $m^{-3} s^{-1} 100 m^{-1}$ represents the offshore Ekman flux in the surface layer. Arrows indicate the days where the in-situ surveys were carried out.

2.2.1. High Performance Liquid Chromatography (HPLC)

For the HPLC chl a determination, water samples (100–200 mL) were filtered through 9 mm diameter Whatman GF/F filters and then stored at -80 °C for two weeks. The pigments were extracted in 95% methanol. In this study only chl a concentration data are presented, calculated as the sum of chlorophyllide a , chlorophyll a epimer, chlorophyll a allomer, and divinyl chlorophyll a . An HPLC method while using a reversed phase C $_8$ was applied for the separation of the pigments. Details of pigment extraction and separation are provided in [58].

2.2.2. Suspended Particulate Material (SPM)

SPM was evaluated in terms of SPM concentration and percent weight of organic material (%OM). Pre-combusted (450 °C for 24 h), pre-washed in 500 mL of MilliQ (Merck, Burlington, MA, USA), and 47 mm Whatman GF/F filters (Merck, Burlington, MA, USA) were used. These filters were then dried at 65 °C to a constant weight. Particles were collected by filtering a standard volume (1000 mL) of seawater samples and then rinsed with 50 mL MilliQ (Merck, Burlington, MA, USA) to remove salts and dissolved organic material. For the determination of SPM, the filters were dried at 65 °C until no weight changes were observed. The filters were then re-combusted at 450 °C for 5 h in order to obtain the inorganic suspended material (ISM) [59,60]. The percent weight of organic material (%OM) was determined by subtracting the ISM from the SPM. All of the filters were weighted on a Precisa 262 SMA-FR microbalance (10⁻⁵ g precision).

2.2.3. Nutrients and Dissolved Organic Carbon (DOC)

The water samples were filtered through 47 mm Whatman GF/F filters (Merck, Burlington, MA, USA) (0.7 µm pore size) and the filtered water was stored at −40 °C for further analysis of DOC and dissolved inorganic micronutrients (nitrate, nitrite, phosphorus, silicate and ammonia). All the nutrients and DOC were analysed with a Technicon AAII (SEAL Analytical GmbH, Norderstedt, Germany) auto-analyser following the methodologies that are described in [61–63]. The ratios of silicate to other nutrients were also calculated due to their importance to marine diatoms.

2.2.4. Particulate Organic Carbon and Nitrogen (POC, PON)

POC and PON content were determined from seawater samples (100–200 mL) filtered through pre-combusted 9 mm diameter Whatman GF/F filters and then stored at −80 °C. The filters were dried at 70 °C and then combusted in a Fisons EA-1108 CHN analyser (Triad Scientific, Inc., Manasquan, NJ, USA) [64]. Sulfanilamide was used as the standard.

2.2.5. *Pseudo-nitzschia* spp. Abundance

We used light microscopy (LM) counting: 250 mL of seawater were fixed with buffered formaldehyde at a final concentration of 1% and stored under dark and cool conditions. An appropriate aliquot (10, 50 mL), depending on the phytoplankton cells density, inorganic suspended material, and detritus density, was settled in a counting chamber. Total abundances of *Pseudo-nitzschia* spp. were enumerated while using an inverted light microscope at 250 × and 400 × magnification [65]. *Pseudo-nitzschia* species were separated into *P. delicatissima* and *P. seriata* complexes depending on their valve width [66].

2.2.6. *Pseudo-nitzschia* Species Identification

Phytoplankton samples for *Pseudo-nitzschia* species identification were collected in the upper 3 m (in order to amass sufficient material for the analysis and to coincide with *Pseudo-nitzschia* spp. LM counting) of each station during the campaigns by vertical net tows with 20 µm mesh-size plankton net. The samples were placed in dark and fixed with paraformaldehyde (to a final concentration of 1%). Scanning electron microscopy (SEM) was performed on selected samples (depending on the presence or not of *Pseudo-nitzschia* in the counting chambers) to identify individual *Pseudo-nitzschia* cells. The removal of the organic matter from the samples involved treatment with hydrogen peroxide and incubation at 90 °C [67]. *Pseudo-nitzschia* species identification was based on the descriptions by [68–70].

2.2.7. Particulate DA (pDA) Analysis

Particulate DA analysis was performed to triplicate sub-samples derived from seawater samples that were collected at the stations shown in Figure 1. The particulate DA retained on the Whatman

GF/F 9 mm filters after the filtration of 200 mL seawater was quantified by ASP cELISA (Biosense Laboratories, Bergen, Norway). A protocol described in [33] was followed for the preparation of the seawater samples and the assay procedure. A Multiskan EX (LabSystems, Bradenton, FL, USA) microplate spectrophotometer with a 450 nm filter was used to read the absorbance of the samples. The detection limit for the ELISA assay was 1 pg DA mL⁻¹ and for the analysis of pDA in the seawater was 0.005 ng DA L⁻¹. The cellular DA (cDA) concentration was calculated by normalizing the pDA concentration to the abundance of *Pseudo-nitzschia* spp. cells that were found in the preserved samples. By pDA we mean how much total domoic acid is present, and by cellular DA (cDA) we refer to how toxic are those cells.

2.2.8. Meteorological Buoys

Meteorological data off the *rias* Baixas were provided by the Spanish Port System (www.puertos.es). Wind speed (W) and direction were observed at a Seawatch buoy station located off Cape Silleiro (42° 7.8'N, 9° 23.4'W). This meteorological station was selected as being representative of the study area [71]. The daily upwelling index (IW) was estimated from wind data according to [72]:

$$IW = -\tau_y/(\rho W \cdot f) = -1000 \cdot \rho_a \cdot CD \cdot W \cdot W_y/(\rho W \cdot f) \text{ (m}^3\text{/(s} \cdot \text{km))} \quad (1)$$

ρ_a is the density of air (1.2 kg·m⁻³ at 15 °C), CD is an empirical dimensionless drag coefficient (1.4·10⁻³ according to [73]), f is the Coriolis parameter (9.9·10⁻⁵ s⁻¹ at 42° latitude), ρW is the density of seawater (1025 kg·m⁻³), and W and W_y are the average daily module and northerly component of the wind, respectively.

2.3. MERIS FR Imagery

Seven full-resolution (FR) level-1b MERIS images that were acquired over the study area between 2007 and 2009 were available in this study. MERIS overpasses were within 2 h of the time that samples and data were collected in situ (Table 1). The MERIS image that was acquired on 7 July 2009 had high cloud coverage and it was removed from the analysis.

Smile correction [74] was applied to the original level-1b data in order to correct the MERIS Top of Atmosphere (TOA) reflectance for the smile distortion, i.e., small variations due to the non-constant central wavelength of a given band across the spectrometer field of view. For the atmospheric correction, the ocean colour data were processed with a neural network (NN)-based algorithm that was developed by [75]. The flags for coastline, land, clouds, and invalid reflectance were raised while using the Beam software to mask the images. Ocean colour data derived from areas significantly affected by sun glint (beyond a solar zenith angle limit of 60°) were also considered invalid and masked. The fuzzy c-mean clustering (FCM) algorithm described by [76] was applied to the MERIS images in order to obtain classification images, in which each open water pixel was assigned to the cluster with the highest value in its corresponding membership function. FCM output includes three clusters with overlapped chl a ranges defining the scope of the regionally specific algorithm for chl a retrieval (neural network for *rias* Baixas-NNRB), which was developed and hence it is only valid for one of the clusters (cluster#1, see [76]). NNRB was finally applied to obtain chl a maps. Both classification images and chl a maps were resampled while using the nearest neighbour method to a common grid (Mercator projection, 890 × 890 pixels) with the same spatial resolution (300 m) as the original images. Each image ranges from 42°04' N to 42°40' N latitude and from 8°32' W to 9°32' W longitude, covering approximately 3.1 × 10³ km².

2.4. Statistical Modelling Approach

Two separate models were developed in this study, which associate *Pseudo-nitzschia* abundance and pDA concentration with selected environmental parameters. Since this diatom includes both toxic and non-toxic species [1], models only based on the abundance might be not always sufficient to

approximate the factors related to toxigenic events. Data exploration showed considerable differences of *Pseudo-nitzschia* spp. density and pDA values between stations and different periods, indicating that these two factors have to be included in the models. Abundance data were analysed while using generalised additive mixed models (GAMMs) that were implemented in the mgcv R package [77]. GAMMs use additive non-parametric functions by smoothing splines to model covariate effects, while allowing correlations between the variables explicitly by adding random effects to the additive variable and they are applicable to nested data structures [78]. Poisson and negative binomial distributions were used for the model fitting of *Pseudo-nitzschia* abundance data, although the negative binomial model did not converge. A linear function was considered and a generalised linear mixed model (GLMM, [79]) was applied to DA concentration data. Gaussian distribution was used for DA data.

Table 2 lists available variables. A square root transformation was applied to *Pseudo-nitzschia* abundance and DA concentration data. Zsd, N (Total Nitrogen, the sum of NO_2^- and NO_3^-), NO_2^- , ISM, Temp, and $\text{Si}(\text{OH})_4/\text{PO}_4^{3-}$ were dropped due to the collinearity that was observed while using the variation inflation factor (VIF) that was computed using the *corvif* function in the AED R package [79]. DOC and pH were also removed from the statistical analysis due to an insufficient number of measurements. The final list of available environmental variables for the GAMMs included Chl a , SPM, Sal, $\text{Si}(\text{OH})_4$, PO_4^{3-} , NO_3^- , NH_4^+ , $\text{Si}(\text{OH})_4/\text{N}$, POC, and PON. Model optimization was based on finding first the optimal random structure and then selecting the optimal fixed structure. Both of the models included each station as a random effect. The final models were selected stepwise on the basis of the AIC (Akaike Information Criterion) and individual significance of explanatory variables. The F test was used to compare the nested models [80]. A multiple regression model was used for the remote sensing-based models.

Table 2. A list of the environmental parameters, units and in-situ mean values during the 3 periods (1: spring downwelling; 2: summer; 3: autumn downwelling). Chlorophyll a (chl a); suspended particulate material (SPM); inorganic suspended material (ISM); Secchi disk depth (Zsd); pH; salinity (Sal); temperature (temp); silicic acid ($\text{Si}(\text{OH})_4$), orthophosphate (PO_4^{3-}); nitrite (NO_2^-); nitrate (NO_3^-); ammonium (NH_4^+), dissolved organic carbon (DOC), particulate organic carbon (POC) and particulate organic nitrogen (PON). nd = not determined, bd = below detection limit (detection limit for: $\text{Si}(\text{OH})_4$: 0.036 mg L^{-1} ; PO_4^{3-} : 0.003 mg L^{-1} ; NO_2^- : 0.001 mg L^{-1} ; NO_3^- : 0.005 mg L^{-1} ; NH_4^+ : 0.001 mg L^{-1} ; DOC: 0.100 mg L^{-1}). We considered only the first 3 m of the depth profiles for pH, salinity and temperature. Square brackets indicate the number of samples for each period.

Parameter	Units	1 (15)	2 (141)	3 (30)
Chl a	$\mu\text{g L}^{-1}$	0.95 ± 0.40	1.24 ± 0.88	3.73 ± 1.71
SPM	mg L^{-1}	1.87 ± 0.15	2.09 ± 0.46	2.47 ± 0.31
ISM	%	37.8 ± 2.9	42.1 ± 11.9	48.5 ± 4.3
Zsd	m	8.8 ± 1.9	6.7 ± 2.7	7.3 ± 1.5
pH	n/a	nd	8.2 ± 0.2	8.1 ± 0.1
Sal	psu	35.5 ± 0.4	33.2 ± 2.6	29.7 ± 0.7
Temp	$^{\circ}\text{C}$	13.1 ± 0.2	18.6 ± 1.1	15.9 ± 0.5
$\text{Si}(\text{OH})_4$	mg-Si L^{-1}	1.380 ± 0.484	0.340 ± 0.091	0.630 ± 0.064
PO_4^{3-}	mg-P L^{-1}	0.606 ± 0.253	0.052 ± 0.126	0.018 ± 0.019
NO_2^-	mg-N L^{-1}	0.354 ± 0.075	0.027 ± 0.039	0.016 ± 0.013
NO_3^-	mg-N L^{-1}	2.689 ± 1.175	0.057 ± 0.120	0.096 ± 0.098
NH_4^+	mg-N L^{-1}	bd	0.009 ± 0.004	0.005 ± 0.002
DOC	mg-C L^{-1}	nd	1.43 ± 0.94	2.98 ± 1.07
POC	mg L^{-1}	0.28 ± 0.08	0.37 ± 0.13	0.33 ± 0.16
PON	mg L^{-1}	0.07 ± 0.00	0.07 ± 0.03	0.04 ± 0.03

3. Results

3.1. Environmental and Meteorological Conditions

Table 2 shows a list of the environmental parameters that were measured in this study and their mean values during the three periods. The surface concentration of nitrates ranged from below detection limit to 3.775 mg L^{-1} and nitrites from 0.005 to 0.415 mg L^{-1} . Highest values for these two macronutrients were observed during the spring downwelling period. Orthophosphate at the sampling stations ranged from below detection limit to 0.850 mg L^{-1} , with high concentrations in the spring downwelling period. Silicic acid concentrations were generally low. The concentration levels of ammonium in surface waters in both studied *rias* were generally low (below 0.023 mg L^{-1}), although elevated ammonium concentrations were observed in the Ria de Vigo during the summer period (22 July 2008). The POC surface concentration varied between 0.13 (autumn downwelling) and 0.75 mg L^{-1} (summer). Higher levels of POC were observed in the summer period (22 July 2008). High concentrations of DOC were found in the autumn downwelling period in accordance with relatively high surface *chl a* concentrations. The SPM concentrations varied from 1.17 to 3.74 mg L^{-1} and the *chl a* values ranged from 0.03 to $6.25 \mu\text{g L}^{-1}$, with a maximum in the autumn downwelling period.

Samples from Ria de Pontevedra revealed higher concentrations of nitrate, nitrite, silicate, and orthophosphate, and the highest concentrations of the three first macronutrients were detected close to the main freshwater inputs in the *ria* (statistically significant at $p < 0.05$ for nitrite and orthophosphate). On the other hand, the ammonium and POC concentrations were generally higher in the Ria de Vigo with statistically significant differences only for ammonium. SPM concentrations showed, in general, decreasing values (in both *rias*) with distance from Station 1, which is located in the inner, narrow part of the *rias* and closer to the main freshwater inputs. In this part of the *rias* sediment resuspension and continental runoff is probably higher, resulting in high concentrations of SPM. ISM followed the same spatial and temporal distribution pattern as SPM. Secchi disk depths ranged from 2 m to 12 m in the Ria de Vigo and from 6 m to 11 m in the Ria de Pontevedra, generally less than half the water column depth.

3.2. *Pseudo-nitzschia* Composition, Abundance, and Particulate Domoic Acid

Scanning electron microscopy observations of the phytoplankton net samples revealed the dominance of *P. australis* Frenguelli (Figure 3). *P. pungens* (Figure 3) and *P. pseudodelicatissima* were also found in the samples. *Pseudo-nitzschia* was recorded during all of the surveys carried out in the study area and it was present in all of the samples. *Pseudo-nitzschia* cells that belonged to the *P. delicatissima* complex were detected in less than one-third of the samples, mainly in lower abundances than the *P. seriata* complex and only when *Pseudo-nitzschia* species belonging to *seriata* complex were present.

In 2008, *Pseudo-nitzschia* spp. were recorded at only few stations and in general with low abundances while pDA was barely detectable in most of the samples (Figure 4). Only *Pseudo-nitzschia* species belonging to *seriata* complex were detected during these campaigns.

During the summer campaign in 2007, the maximum abundance of *Pseudo-nitzschia* spp. ($> 0.44 \cdot 10^4 \text{ cells L}^{-1}$) in the Ria de Vigo was detected at the station 1, located at the innermost part of the *ria*.

In 2009, *Pseudo-nitzschia* spp. abundances in the Ria de Pontevedra averaged 80 cells L^{-1} on May 27 and $0.40 \cdot 10^4 \text{ cells L}^{-1}$ on July 7. pDA values in all of the samples from the Ria de Pontevedra were above the detection limit, but relatively low (0.01 – $0.07 \mu\text{g L}^{-1}$). The cellular DA levels varied from 0 to $54.31 \text{ pg DA cell}^{-1}$ (Figure 4) *Pseudo-nitzschia* spp. abundance almost linearly decreased from the warm surface waters (around $19 \text{ }^\circ\text{C}$) at the inner part of the Ria de Vigo to the colder ($17 \text{ }^\circ\text{C}$) more saline waters outside the *ria*. In order to investigate the dominant conditions during toxic blooms in more detail, the toxic *Pseudo-nitzschia* events have also been individually studied in Section 3.3.

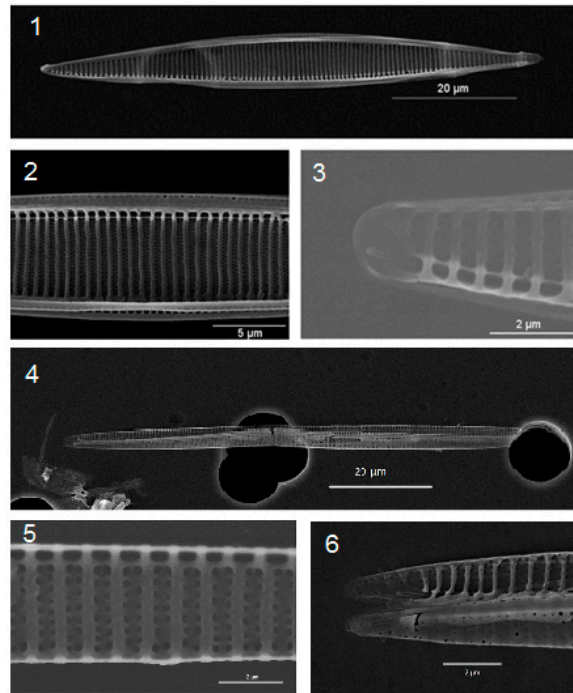


Figure 3. (1–3) Scanning electron micrographs of *Pseudo-nitzschia australis*. Note the: (1) apically asymmetric valve; (2,3) details of the rounded poroids arranged in two striae, the absence of central interspace. (4–6) Scanning electron micrographs of *P. pungens*. Note the: (4) Linear to lanceolate valves (5,6) 2 rows of poroids in contact with interstriae and arranges in opposite sites. Scale bar: (1) 20μm, (2) 5μm, (3) 2μm, (4) 20μm, (5) 2μm, and (6) 2μm.

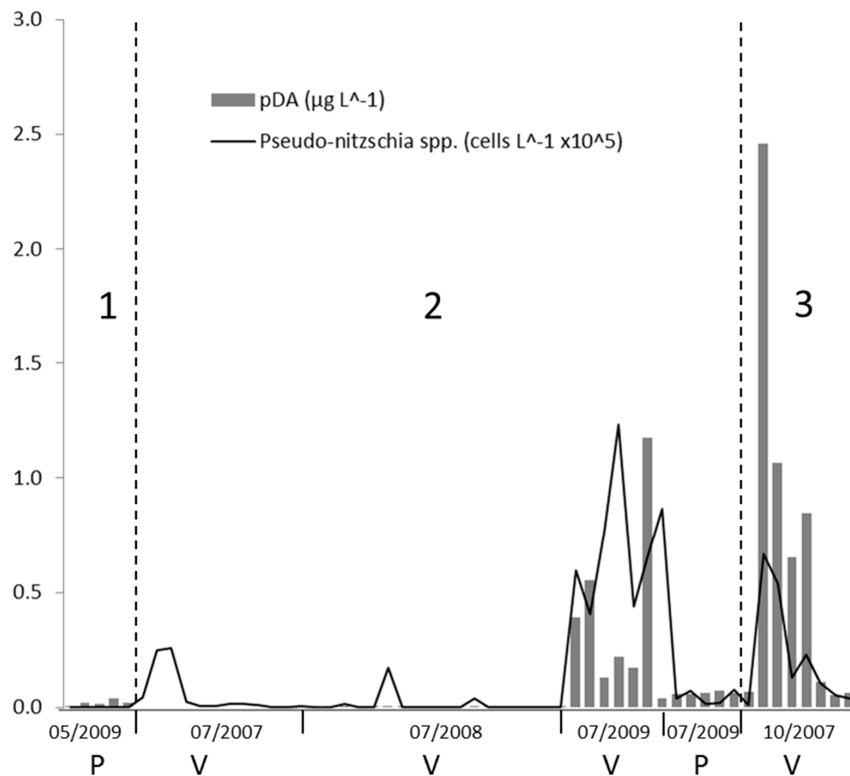


Figure 4. Abundance of *Pseudo-nitzschia* spp. plotted with concentration of pDA across all the stations in Ria de Vigo (V) and Ria de Pontevedra (P) during our sampling period for periods (1) (spring downwelling), (2) (summer), and (3) (autumn downwelling).

3.3. *Pseudo-nitzschia* Toxic Events

The first toxic event was recorded in the autumn downwelling period (19/10/2007) in the Ria de Vigo during a downwelling period. It was characterised by high abundances of *Pseudo-nitzschia* spp. that belonged to the *seriata* complex and DA concentrations up to 2.51 $\mu\text{g L}^{-1}$. Surface pDA was detectable at all of the sites with available samples. pDA concentrations were higher than 0.50 $\mu\text{g L}^{-1}$ throughout the middle part of the Ria de Vigo and they were still detectable, but in lower concentrations (close to 0.05 $\mu\text{g L}^{-1}$) outside and at the inner part of the *ria* (Figure 5). pDA in the Ria de Vigo showed a strong positive significant relationship with *Pseudo-nitzschia* spp. in this dataset (Pearson's $r = 0.92$, $p = 0.001$). *Pseudo-nitzschia* spp. abundances and pDA concentrations were also highly correlated with Secchi disk depth ($r = -0.75$), TSM ($r = -0.83$), POC ($r = 0.87$), chl a ($r = -0.77$), and the ratios of $\text{Si(OH)}_4/\text{PO}_4^{3-}$ ($r = -0.72$) and $\text{Si(OH)}_4/\text{N}$ ($r = -0.71$) (Table 3). For the same survey, mean cellular DA was 31.7, ranging between 9.5 and 70.30 pg DA cell $^{-1}$. The highest cellular DA concentration was recorded at the site (V1) where the lowest *Pseudo-nitzschia* spp. abundance (0.1 10^4 cells L^{-1}) was found.

Table 3. Pearson's correlations between *Pseudo-nitzschia* spp. abundances (P-N in cells L^{-1}), particulate DA (pDA in $\mu\text{g L}^{-1}$), and cellular DA (cDA in pg DA cell $^{-1}$) concentrations with several environmental parameters during 10 October 2007 and 14 July 2009.

10 October 2007							
	pDA	Chl a	SPM	Zsd	pH	Sal	Si(OH)_4
P-N	0.92 **	0.77 *	0.83 *	-0.75 *	0.20	-0.09	-0.49
pDA		0.67	0.78*	-0.69	0.07	0.04	-0.44
cDA		0.36	0.28	-0.22	-0.23	-0.62	0.26
	Temp	PO_4^{3-}	N	$\text{Si(OH)}_4/\text{PO}_4^{3-}$	$\text{Si(OH)}_4/\text{N}$	POC	
P-N	0.16	-0.02	0.00	-0.72 *	-0.71 *	0.87 *	
pDA	0.32	-0.32	0.02	-0.71 *	-0.69	0.84 **	
cDA	0.83 *	0.51	0.09	-0.24	0.00	-0.24	
14 July 2009							
	pDA	Chl a	SPM	Zsd	pH	Sal	Si(OH)_4
P-N	-0.08	0.11	0.66	-	-	-0.46	0.01
pDA		-0.24	-0.15	-	-	0.67	0.00
cDA		-0.06	-0.70	-	-	0.50	0.00
	Temp	PO_4^{3-}	N	$\text{Si(OH)}_4/\text{PO}_4^{3-}$	$\text{Si(OH)}_4/\text{N}$	POC	
P-N	0.28	-0.33	-0.59	-0.23	0.75 *	0.03	
pDA	-0.52	0.02	0.21	-0.03	-0.28	0.48	
cDA	-0.43	0.71	0.96 **	-0.16	-0.92 **	0.22	

* significant at $p < 0.05$ and ** significant at $p < 0.001$.

On 14 July 2009 (summer period), a toxic event mostly due to *Pseudo-nitzschia seriata* complex was monitored in the Ria de Vigo. During this event, *Pseudo-nitzschia* spp. reached the highest abundance for the sampling period in the area ($12 \cdot 10^4$ cells L^{-1}). *Pseudo-nitzschia* abundance was high at all sites averaging $5.65 \cdot 10^4$ cells L^{-1} . pDA was detectable in all of the samples and ranged between 0.04 to 1.18 $\mu\text{g L}^{-1}$. The highest pDA concentrations were found in samples from sites close to the southern mouth of Ria de Vigo while the lowest concentration was recorded close to the northern mouth of the *ria* (Figure 5). The maximum pDA concentration for this sampling was measured in a sample containing $6.90 \cdot 10^4$ cells L^{-1} of *Pseudo-nitzschia* spp., while the minimum pDA concentration was found in a sample that contained the same magnitude of *Pseudo-nitzschia* spp. ($5.62 \cdot 10^4$ cells L^{-1}). Cellular DA concentrations averaged 14.20 pg DA cell $^{-1}$, showing a wide range of values (0.70–58.62 pg DA cell $^{-1}$). There was no significant correlation (Pearson's test) between *Pseudo-nitzschia* spp., DA concentration and cellular DA concentration for this sampling. *Pseudo-nitzschia* spp. abundance was positively

correlated to the $\text{Si}(\text{OH})_4/\text{N}$ ratio ($r = 0.75$, $p = 0.05$), while a strong relationship was revealed between the cellular DA concentration and N ($r = 0.96$) and $\text{Si}(\text{OH})_4/\text{N}$ ($r = -0.92$) (Table 3).

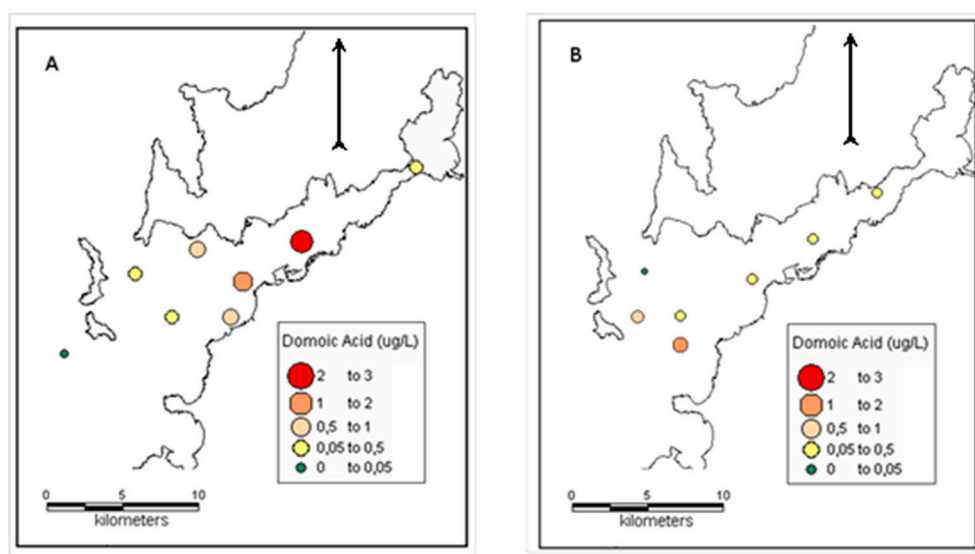


Figure 5. Distribution of particulate domoic acid (pDA) during the two high DA episodes recorded in the surface waters of Ria de Vigo on (a) 19 October 2007 and (b) 14 July 2009.

3.4. Remote Sensing Detection

The FCM clustering method was applied in available MERIS FR images to build classification images defining the scope of the regionally specific algorithm for *chl a* retrieval (NNRB). These images revealed large areas where Cluster#1 is dominant, and therefore NNRB could be applied to obtain reliable results of *chl a* concentration. Table 4 shows the percentage of pixels that belong to each cluster for each image over the Ria de Vigo and Ria de Pontevedra. Cluster#1 was dominant in both *rias*, averaging almost 92% of the pixels in the six images, while Cluster#2 and Cluster#3 were assigned to an average of 7.9% and 0.3% of the pixels, respectively.

Table 4. Percentage of pixels belonging to each cluster over the study area, obtained from classification images derived from the MERIS images used in this study.

Date	ria	Cluster#1	Cluster#2	Cluster#3
25 July 2007	Vigo	98.53	0.92	0.55
	Pontevedra	99.70	0.30	0.00
10 October 2007	Vigo	97.70	2.30	0.00
	Pontevedra	97.93	1.48	0.59
9 July 2008	Vigo	95.40	4.04	0.55
	Pontevedra	96.14	3.57	0.30
22 July 2008	Vigo	87.41	11.88	0.71
	Pontevedra	90.06	9.79	0.15
27 May 2009	Vigo	98.07	1.58	0.35
	Pontevedra	98.98	1.02	0.00
14 July 2009	Vigo	70.59	29.01	0.41
	Pontevedra	71.20	28.51	0.29

In most of the images, Cluster#1 is dominant, allowing for the *chl a* mapping over large areas. Only on 14 July 2009, the relatively high percentage of pixels belonging to Cluster#2 in combination with the cloud cover averted a reliable continuous *chl a* mapping of the *rias*.

Spatial distribution of phytoplankton biomass in the study area was analysed from the available MERIS FR images while using the NNRB *chl_a* algorithm, showing heterogeneous results (Figure 6). Elevated *chl_a* concentrations in the shallow innermost parts of the *rias* observed in some images are most likely due to the high abundances of macroalgae on the remote sensing signal since in-situ measurements showed generally lower values.

On 25 July 2007, MERIS NNRB surface *chl_a* concentrations were relatively low ($<1 \mu\text{g L}^{-1}$) in most parts of the Ria de Vigo and Ria de Pontevedra. An area of *chl_a* concentrations close to $2.5 \mu\text{g L}^{-1}$ was mapped in the area off the external coast of the *rias*. Generally, surface *chl_a* concentration was higher in offshore areas, where the lowest concentrations of *Pseudo-nitzschia* spp. were found.

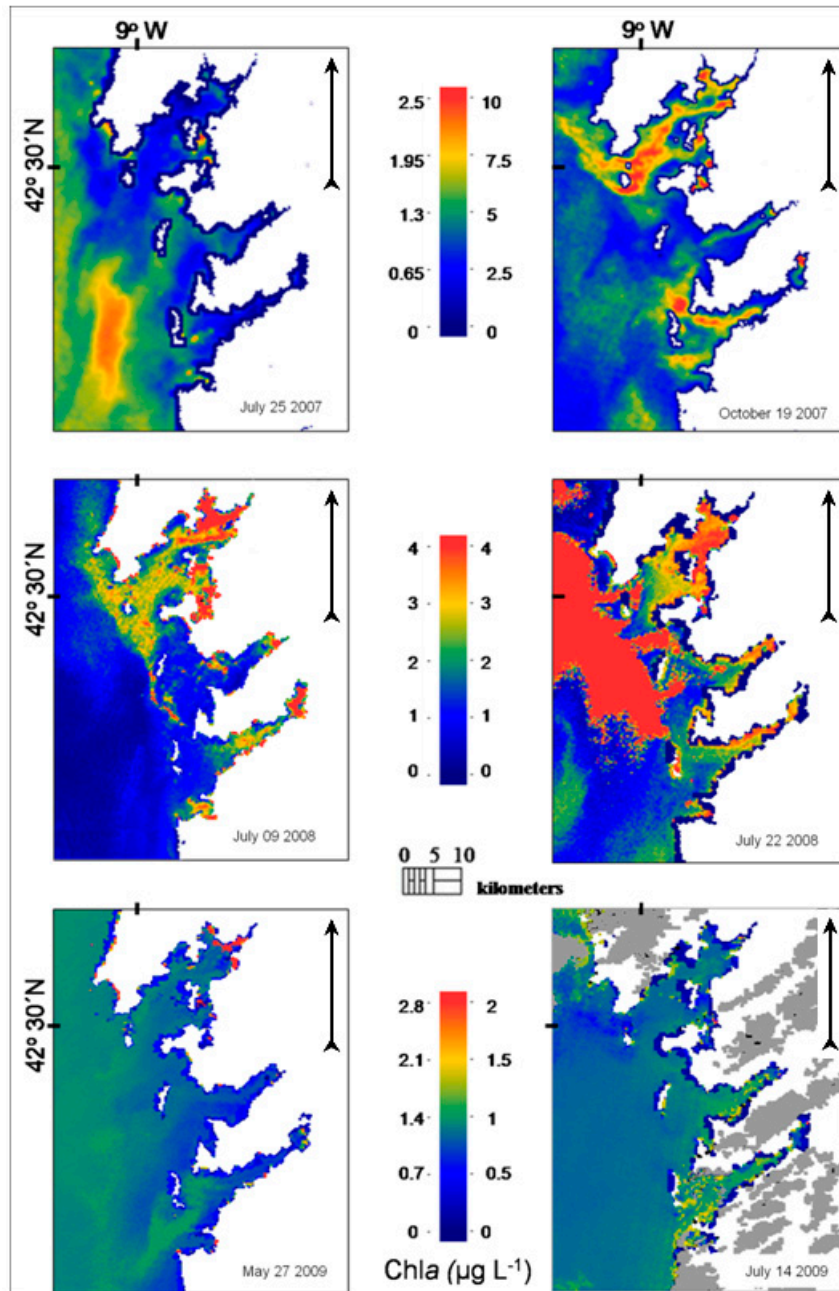


Figure 6. Chl_a maps retrieved from MERIS full-resolution (FR) data using the neural network for *rias* Baixas (NNRB) on the survey dates. White colour indicates masking of land while grey masking of clouds. Pixels belonging to Cluster#2 and Cluster#3 were assigned a value of 0 (dark blue).

Maximum MERIS NNRB *chl a* concentrations were observed on 19 October 2007 coinciding with the first toxic event recorded during the sampling period and related to the presence of *Pseudo-nitzschia* spp. in the Ria de Vigo. In fact, the *chl a* map shows high biomass “patches” clearly defined in this *ria*, i.e., zones of elevated *chl a* concentrations (up to $10 \mu\text{g L}^{-1}$) at the middle part, just where the highest *Pseudo-nitzschia* spp. concentrations were measured, and also close to the northern and southern mouths. In the Ria de Pontevedra, the *chl a* concentration was significantly lower in comparison with the concentrations observed in the Ria de Vigo and the Ria de Arousa. Areas of relatively high *chl a* concentrations were noted in the adjacent area of the *rias*.

In the next MERIS image, which was acquired on 9 July 2008, a different *chl a* distribution pattern is observed: the phytoplankton biomass is principally confined in the *rias*, while in the area off the *rias* the *chl a* concentration remained at levels close to $0 \mu\text{g L}^{-1}$.

On 22 July 2008, high *chl a* concentrations were mapped in the neighbouring shelf area. High concentrations were also extended to the outside part of Ria de Arousa and Ria de Pontevedra. The *chl a* that was retrieved by NNRB in the Ria de Vigo showed wider variation than the concentrations measured in situ. During July 2008 *Pseudo-nitzschia* abundances remained at low levels.

On 27 May 2009, concentrations of *chl a* lower than $1 \mu\text{g L}^{-1}$ were mainly noted in the three southern *rias*, while NNRB estimates were above this value off the *rias*. Low *chl a* concentrations close to or lower than $1 \mu\text{g L}^{-1}$ were also observed both on the adjacent continental shelf and inside the *rias* on 14 July 2009.

The results of the multiple regression indicated that spectral reflectance in MERIS bands centred around 510 (Rrs_510), 560 (Rrs_560) and 620 (Rrs_620) nm explain 73% of the pDA variance ($R^2 = 0.73$, $F_{(2,32)} = 32.26$, $p < 0.001$). It was found that Rrs_510 significantly predicted pDA ($\beta = 0.31$, $p < 0.001$), as did Rrs_560 ($\beta = -1.56$, $p < 0.01$) and Rrs_620 ($\beta = 3.24$, $p < 0.001$).

3.5. Model Results of *Pseudo-nitzschia* spp. and pDA as a Function of Biotic and Abiotic Parameters

The results of generalised additive mixed models (GAMMs), which were used to model *Pseudo-nitzschia* abundances in response to biotic and abiotic parameters, are summarised in Table 5. The GAMMs results show a significant ($p < 0.005$) linear relation of salinity and *chl a* with *Pseudo-nitzschia* abundance. The optimal model fitted the ratio $\text{Si(OH)}_4/\text{N}$ in an additive way ($p = 0.02$). The cross-validation estimated the degrees of freedom for this function to be 3.08. The smoothing curve that is shown in Figure 7 suggests a peak of *Pseudo-nitzschia* spp. abundance in moderate values of the $\text{Si(OH)}_4/\text{N}$ ratio (close to 1.7) and an almost linear decrease for higher values. From all of the explanatory variables that were tested to model the pDA concentration, the final GLMM model included POC ($p = 0.02$), NO_3^- ($p = 0.03$), PO_4^{3-} ($p = 0.004$), and $\text{Si(OH)}_4/\text{N}$ ($p = 0.02$). Parameters estimates with SE and *t*-values for the linear covariates are given in the Table 6. Examination of the residuals did not indicate patterns.

Table 5. Results of the generalised additive mixed models used to model the *Pseudo-nitzschia* spp. as a function of biotic and abiotic parameters. For linear covariates the parameter estimates with SE and *t*-values are given. For the additive covariate the estimated degrees of freedom (edf) and F-value are provided. Periods 1 (spring downwelling), 2 (summer), and 3 (autumn downwelling) corresponds to May, July, and October.

Period	Estimates	SE	<i>t</i>
1	−6.85	±2.83	−2.42
2	3.01	±1.72	1.74
3	3.73	±1.82	2.05
Linear effects	Estimates	SE	<i>t</i>
Sal	0.21	±0.06	3.39
chl <i>a</i>	0.89	±0.31	2.90
Additive effects	edf	F	
Si(OH) ₄ /N	3.08	3.61	

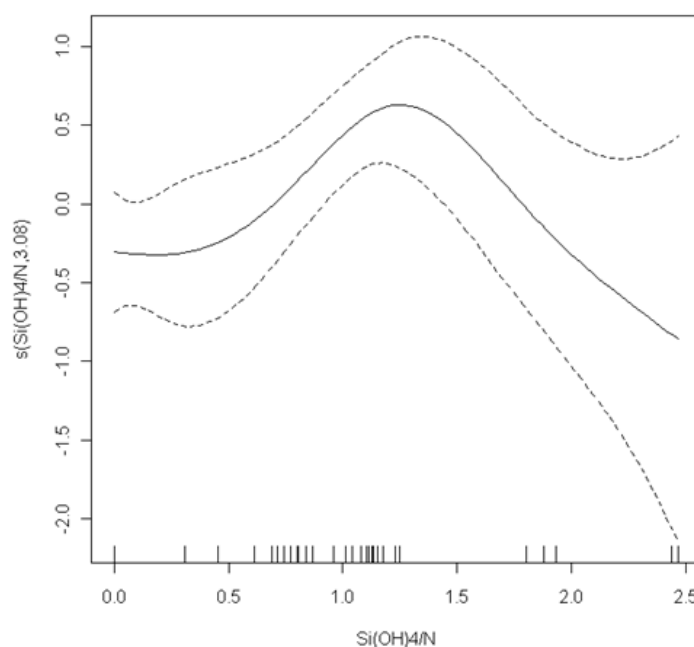


Figure 7. Generalised additive mixed model (GAMM) results: model of *Pseudo-nitzschia* spp. abundance: smoothers and estimated degrees of freedom (*y* axis) showing partial effects of Si(OH)₄[−]:N ratio on *Pseudo-nitzschia* spp. abundance. *x* axis in cubic root (mg-N L^{−1}).

Table 6. Results of the best generalised linear mixed model that shows the effect of abiotic and biotic parameters on particulate domoic acid (pDA) in our database. Station was included as random effect. Parameter estimates with SE and *t*-values are given. Periods are the same as in Table 4.

Period	Estimates	SE	<i>t</i>
1	−0.12	0.29	0.42
2	0.09	0.23	0.39
3	0.79	0.26	3.07
Parameters	Estimates	SE	<i>t</i>
POC	0.70	0.29	2.42
NO ₃ [−]	−0.38	0.17	−2.23
PO ₄ ^{3−}	0.69	0.22	3.15
Si(OH) ₄ /N	−0.18	0.07	−2.51

4. Discussion

4.1. *Pseudo-nitzschia* Abundance and Species

Pseudo-nitzschia spp. were revealed to be a common component of the phytoplankton assemblages during the summer period in the study area, since they were recorded in the samples from all summer surveys. Concomitantly, in their review on HABs in upwelling areas, Trainer et al. [26] reached a similar conclusion that *Pseudo-nitzschia* spp. are present in the Galician *rias* mainly during late spring-summer. Nevertheless, we recorded an autumn-time high abundance event in the Ria de Vigo. The *Pseudo-nitzschia* assemblages during our study mostly contained *Pseudo-nitzschia* species belonging to the *seriata* complex. *Pseudo-nitzschia* species belonging to the *delicatissima* complex were also present in some samples and always along with *Pseudo-nitzschia seriata* complex species. *P. australis* was identified as the dominant species in the net (selected) samples that were examined by electron microscopy. However, field samples from both *rias* contained *P. delicatissima* and *P. pungens* cells. The latter species is an important part of the phytoplankton community in the Ria de Pontevedra during late winter and summer upwelling/downwelling conditions [81].

4.2. Domoic Acid

The present study provides DA concentrations from natural phytoplankton populations in the Galician *rias*. The results of this survey show that relatively high *Pseudo-nitzschia* spp. abundances and DA concentrations can be distributed throughout the surface waters of Ria de Vigo. Overall, pDA was detected in more than half of the samples that were obtained during the surveys (2007–2009) and relatively high values of pDA and cDA were found. In our data, pDA ranged from below detection limits to $2.51 \mu\text{g L}^{-1}$. Similar pDA levels have been measured in the surface waters in other coastal upwelling areas around the world, where *P. australis* was the dominant *Pseudo-nitzschia* species during the blooms [27,82–84]. For example, the same magnitude of *Pseudo-nitzschia* abundance ($7 \cdot 10^4$ cells L^{-1}) that gave us the maximum pDA concentration ($2.51 \mu\text{g L}^{-1}$) was detected in San Diego (USA), where the pDA levels reached $2.3 \mu\text{g L}^{-1}$ [82]. Cellular DA in the field samples varied between 0 and $70.30 \text{ pg DA cell}^{-1}$. We are not aware of other measurements of cellular DA content in field populations from the Iberian upwelling system. Several studies along the West coast of USA have recorded analogous ranges of cellular DA during harmful events, which were mainly due to *P. australis* ($7\text{--}75 \text{ pg DA cell}^{-1}$: [85]; $0.1\text{--}78$: [36]; $5\text{--}43 \text{ pg DA cell}^{-1}$: [82]; $0.14\text{--}2.1 \text{ pg DA cell}^{-1}$: [9]; and, $0\text{--}117 \text{ pg DA cell}^{-1}$: [27]). From the two toxic *Pseudo-nitzschia* events recorded in our study, cDA was higher in the Ria de Vigo on the 19 October 2007. According to the data from INTECMAR (www.intecmar.gal), *Pseudo-nitzschia* population in this *ria* was in the declining phase. This is consistent with numerous (e.g., [86]) reports of increased cDA at the late stages of the population. The second toxic event found the *Pseudo-nitzschia* close to the peak of abundance.

4.3. *Pseudo-nitzschia* spp. Toxic Events in the Study Area and ASP Implications

In our study, the first toxic event in the Ria de Vigo was recorded on 19 October 2007. It was characterised by high pDA concentrations due to moderate abundances of *Pseudo-nitzschia*. It is worth mentioning that high *Pseudo-nitzschia* spp. abundances have been previously observed in the Galician *rias* during autumn causing the closure of the mussel harvesting beds [12].

In our data, a second DA episode due to *Pseudo-nitzschia* spp. was recorded in the Ria de Vigo on 14 July 2009, but showing lower pDA concentrations. INTECMAR also found high *Pseudo-nitzschia* spp. abundances (over 10^5 cells/L) in the *rias* during the last three weeks of July 2009, although closures of mussel rafts polygons were mainly associated with the presence of DSP (Diarrhetic Shellfish Poisoning), while DA data were not available.

In the same year, Pazos and Morono [87] observed very high abundances of *P. australis* in May in the Rias de Vigo and Pontevedra over a week. Raft mussels and natural shellfish beds closures due to ASP (Amnesic Shellfish Poisoning) were reported in Rias of Pontevedra and Vigo from late March to

early April, whereas DA was found above the regulatory levels in scallops (*Pecten maximus*) during the whole 2009 as well as 2007 [88,89].

In the situations that are described above, it seems that, even if we detected high concentrations of pDA (up to $2.51 \mu\text{g L}^{-1}$) in our survey in 2007, DA in mussels was below regulatory levels during the whole year. Likewise, in 2009, despite the high pDA detected during our campaigns, DA was not taken up by the suspended mussel raft cultures. A possible explanation for this could be either rapid depuration or the result of food selection or dilution [90–93]. Another factor that might be associated with the observed situation, where mussels do not seem to take up the DA, despite the high pDA concentrations, is the possible short-term duration of these harmful events. Spyrakos et al. [53] describe using remote sensing data important changes on phytoplankton biomass in the *rias* within three days and highlight the challenges for the detection and monitoring of harmful algal events in a physically complex system, such as the Galician *rias*. Nonetheless, even these short-term high DA events, if they are recurrent, can pose a significant threat to the harvesting of species that show slow DA depuration rates, like scallops [94,95].

Diaz et al. [96] analysed phytoplankton and mussel samples that were collected from the Ria de Pontevedra from 28 May to 7 June 2007, and despite the high abundances of *Pseudo-nitzschia* spp. (higher than 5×10^5 cells L^{-1}) with the dominance of *P. australis* were observed, DA analysis using HPLC-UV methods did not reveal any detectable concentrations in the seawater or above regulatory levels in mussels. Discrepancies that were observed in our DA data in comparison to those by [95] and INTECMAR could be also due to the different methods, followed by the quantification of DA. ELISA methods have shown more sensitive detection limits for DA than HPLC-UV based methods and appear to perform better in the formalin-fixed samples [97,98]. However, overestimation has been observed in some cases [49] while using ELISA in the quantification of DA. This overestimation was attributed to the detection by the antibodies of domoic acid isomers in addition to the domoic acid and epi-domoic acid.

4.4. Environmental Conditions Associated with *Pseudo-nitzschia* spp. Abundance and DA Concentration

This study attempts to provide insight on the environmental conditions that are associated to the occurrence of toxic *Pseudo-nitzschia* spp. events in the surface waters of two Galician *rias*. González Vilas et al. [14] while using a larger database of *Pseudo-nitzschia* spp. abundances, but with limited environmental factors discussing possible processes related to high abundances of these diatoms in the area. Here we attempt to get a better understanding on the relationships between the measured parameters and the toxic *Pseudo-nitzschia* events, which may be essential for future monitoring and prediction efforts. Due to considerable differences in the *Pseudo-nitzschia* spp. abundance and pDA concentration among the three different periods of dominant meteorological conditions off the *rias*, these periods were included in the models as a variable. The results show that there is higher probability of high *Pseudo-nitzschia* spp. abundance and pDA in the summer period (summer upwelling-downwelling cycle) and the autumn downwelling period (autumn strong downwelling) (Tables 5 and 6). These results are consistent with previous studies on *Pseudo-nitzschia* spp. abundance in upwelling systems [99].

Results of GAMMs for *Pseudo-nitzschia* spp. revealed a significant linear effect (refers to statistical relationships and not biogeochemical processes) of salinity, chl a , and the additive effect of the Si(OH) $_4$ to N ratio. The preference of *Pseudo-nitzschia* spp. for higher values of salinity found in our dataset confirms previous observations on *Pseudo-nitzschia* spp. in coastal waters of Galicia. For example, [100] analysed time series of *Pseudo-nitzschia* spp. abundance between 1999 and 2000 and concluded that *Pseudo-nitzschia* spp. blooms were mainly recorded in high salinity values (> 35). Salinity has been suggested as an important regulator of specific *Pseudo-nitzschia* species or *Pseudo-nitzschia* spp. abundance in other observational studies around the world (e.g., Adriatic Sea: [41]; West Coast of USA: [26]; Gulf of Mexico: [29]; and, Sea of Marmara: [23]).

The final GAMM fitted to the *Pseudo-nitzschia* spp. abundance includes linear relationship with chl a . [8,36,37] pointed out that there is higher probability for *Pseudo-nitzschia* spp. blooms when chl a concentration is high. The trend observed during the sampling period of higher *Pseudo-nitzschia* spp. abundances with high chl a concentrations can be valuable in the remote sensing detection of high biomass “patches” in the Galician rias.

According to GAMM results, *Pseudo-nitzschia* spp. abundance increases until a maximum value at moderate values of the ratio of Si(OH) $_4$ to N (mainly NO $_3^-$), followed by a sharp decline at higher values. These results suggest that lower, but not the lowest, ratio values favour higher *Pseudo-nitzschia* spp. abundances. The results support the consideration that silicate and inorganic nitrogen are limiting factors for the growth of several *Pseudo-nitzschia* species [9,27–31,39,86]. Schnetzer et al. [27] also suggested that the observed decline of Si concentrations when the *Pseudo-nitzschia* spp. abundances are high could be explained by the fact that samplings can occur after the growth of *Pseudo-nitzschia*, and hence Si has been drawn down.

Nutrient availability at the end of the blooms has been suggested as possible factor that is implicated in the appearance of toxic *Pseudo-nitzschia* spp. events in the Galician rias [26,101]. However, the environmental conditions that are related to the pDA occurrence and distribution in the area are poorly defined. The GLMM identified POC, NO $_3^-$, PO $_4^{3-}$, and Si(OH) $_4$ /N as significant factors that influence pDA concentration. The enhancement of higher pDA concentrations by low Si(OH) $_4$ /N observed in our data are consistent with the results that were reported in [9] in the Santa Barbara Channel, California, and in other field studies in which DA seems to be associated with Si-limitation [7].

Moreover, our results (Table 6) showed that the PO $_4^{3-}$ and NO $_3^-$ concentrations have a significant effect on the pDA in the surface seawater. The relationship between DA production by several *Pseudo-nitzschia* species and the availability of these two macronutrients has been studied in several laboratory experiments [30,31,33,102,103]. In some of these laboratory studies, PO $_4^{3-}$ -limitation and N-sufficiency (since DA is an amino-acid) have been pointed out as the driving factors for DA production. Contradictorily, in our study, moderate-high pDA values were found in relatively high PO $_4^{3-}$ and low NO $_3^-$ concentrations. This is possibly implicating the necessity to consider other environmental conditions, which might be responsible for the production of DA, as it is also suggested by field studies [7,104,105].

The final GAMM fitted to the *Pseudo-nitzschia* spp. abundance includes the linear effect of chl a . This probably reflects a dominance or co-dominance of *Pseudo-nitzschia* spp. in the phytoplankton community. Several studies [8,36,37] suggest a relationship between high chl a concentrations and the occurrence of *Pseudo-nitzschia* spp. blooms.

5. Summary & Concluding Remarks

Domoic acid (DA) was measured in the seawater samples from the Galician rias and revealed the presence of high levels in several cases. DA concentrations were not always related to *Pseudo-nitzschia* abundances, showing that cell counts are not enough for assessing the toxicity of *Pseudo-nitzschia* occurrence in the area. Despite the fact that no serious illnesses that were caused by ASP were reported in the area (Intecmar, Ministerio de Sanidad y Consumo) during the study period, DA levels, such as the ones detected here, could have the potential for significant impacts on the ecosystem and human health (e.g., by chronic exposure to moderate toxin levels, as it is mentioned by [106] and [107]). Furthermore, the DA content in some potential vectors that can be consumed by humans and other marine animals has not been studied in the Galician rias.

In this study, mixed effect modelling was used to associate several environmental factors with the toxic *Pseudo-nitzschia* events for three different seasonal upwelling-downwelling conditions. The major aspects of phytoplankton succession in the area are relatively well known, in terms of major groups (diatoms, dinoflagellates, flagellates). Here, we intended to obtain to a finer degree of resolution, focusing in a particular group of diatoms. The results show that higher salinity values and lower, but not the lowest, Si(OH) $_4$ /N ratios favour higher *Pseudo-nitzschia* spp. abundances. High pDA

values seem to be associated with relatively high PO_4^{3-} , low NO_3^- concentrations, and low $\text{Si}(\text{OH})_4/\text{N}$. Knowledge of these relationships could help in evaluating the potential impacts of the blooms due to *Pseudo-nitzschia* on mariculture and wildlife, and improve our ability to predict toxic events as a function of environmental parameters.

The relationships that were found by the models only apply to the study area and the data that were collected during this period. Longer time-series from a wider area, samples from discrete depths, and micronutrients data could offer more detailed insight regarding the occurrence of toxic *Pseudo-nitzschia* spp. events. Nevertheless, this study documents the presence of toxigenic *Pseudo-nitzschia* and suggests that the monitoring of DA in the natural populations of *Pseudo-nitzschia* could be useful for identifying potential risks for DA contamination into higher trophic levels. Further research is also needed in the pathways of DA to higher trophic levels and examination of the relationships between *Pseudo-nitzschia* spp. blooms in the area and closures of mussel farms due to DA.

In this study, chl a is retrieved from MERIS FR data while using a regional algorithm previously developed [75]. A part of the chl a data from the surveys described here has been used for the development of this regional neural network-based algorithm, which has been shown to permit the accurate mapping of chl a of the rias [53]. In our MERIS imagery set, Cluster#1 was dominant in the three rias and the adjacent area allowing for reliable chl a mapping over the area. The autumn-time DA event was characterised by high chl a concentrations. The highest *Pseudo-nitzschia* spp. abundances (3 to 6 10^4 cells L^{-1}) were found in a relatively small area in the Ria de Vigo where elevated surface chl a concentration (>6 mg m^{-3}) was mapped from the MERIS FR data. These small areas of high chl a concentration accompanied with moderate abundances of toxic *Pseudo-nitzschia* spp. can be easily missed by conventional monitoring techniques. The MERIS FR and MODIS (not shown here) images from the extended area of the Iberian Peninsula show very high chl a concentrations, coupled with colder waters along the Portuguese and Galician coast indicating a general high biomass event.

Moreover, our results show “patchiness” in the spatial distribution of *Pseudo-nitzschia* in this coastal upwelling system, which suggests that the spatial and temporal resolution for the monitoring of these events should be increased. Ocean colour techniques can be helpful in tracking potentially harmful events that are caused by *Pseudo-nitzschia* and complement monitoring programs based on direct observations at fixed stations. Satellite data can be even more useful following the approach of this study with near real-time fine resolution imagery and regionally/cluster-specific algorithms for the retrieval of chl a concentrations. According to the recorded in situ data, our approach to retrieve chl a is an improvement on other previously used techniques, and made it possible to obtain reliable chl a maps while using almost every image. The relationship that was established in this paper between the MERIS Rrs and pDA can be the basis of an effective Earth Observation (EO)-based HAB monitoring that will address the requirements of several key regional end-users.

Another finding is the relationship between MERIS FR data and pDA. In a previous study, Anderson et al. [108] also developed regression models for *Pseudo-nitzschia* spp. abundance, pDA, and cDa in the Santa Barbara channel integrating ocean colour (MODIS-Aqua and SeaWiFS) and sea surface temperature (AVHRR) data, finding relationships while using similar spectral bands (510 nm and 555 nm). Although our model is based on a limited dataset and it requires further research, it could be a good starting point for the development of new algorithms for the Rias Baixas area.

Although the Envisat satellite has stopped functioning in May 2012, the approach that was followed with MERIS by the authors could be adapted to other satellite-based ocean colour sensors. At present, we are involved in the European (EU H2020) funded project CoastObs [109], which explores the potential use of the new Sentinel satellites to monitor coastal water environments. It includes, among its objectives, the development of validated map products that were derived from Sentinel 3 images that are expected to provide useful information for HABs detection and monitoring in Galicia, including not only chl a concentration, but also species indicators for specific species, such as *Pseudo-nitzschia* spp. or *Alexandrium minutum*.

Author Contributions: Conceptualization, J.M.T.P., F.M.B. and E.S.; methodology, E.G., A.G.-F. and E.S.; formal analysis, e.g., A.G.-F. and E.S.; resources, J.M.T.P. and A.G.-F.; writing—original draft preparation, J.M.T.P., E.G., A.G.-F. and E.S.; writing—review and editing, F.M.B., L.G.V. and E.S.; visualization, L.G.V. and E.S.; supervision, J.M.T.P. and E.S.; project administration, J.M.T.; funding acquisition, J.M.T. and E.S.

Funding: This study was funded by the European Union’s Horizon 2020 research and innovation programme (grant agreement n° 776348) and Marie Skłodowska-Curie Actions (project 20501 ECOSystem approach to Sustainable Management of the Marine Environment and its living Resources (ECOSUMMER)).

Acknowledgments: We are very grateful to A. Acuña and D. Perez Estevez for their helpful assistance during the fieldwork. We also thank Aldo Barreiro for his useful comments on the manuscript.

Conflicts of Interest: The authors declare no conflict of interest.

References

1. Hasle, G.R. Are most of the domoic acid-producing species of the diatom genus *Pseudo-nitzschia* cosmopolites? *Harmful Algae* **2002**, *1*, 137–146. [[CrossRef](#)]
2. Bates, S.S.; Garrison, D.L.; Horner, R.A. Bloom dynamics and physiology of domoic-acid-producing *Pseudo-nitzschia* species. In *Physiological Ecology of Harmful Algal Blooms*; Anderson, D.M., Cembella, A.D., Hallegraeff, G.M., Eds.; Springer: Berlin, Germany, 1998; Volume 41, pp. 267–292.
3. Quiroga, I. *Pseudo-nitzschia* blooms in the Bay of Banyuls-sur-Mer, northwestern Mediterranean Sea. *Diatom Res.* **2006**, *21*, 91–104. [[CrossRef](#)]
4. Terseleer, N.; Gypens, N.; Lancelot, C. Factors controlling the production of domoic acid by *Pseudo-nitzschia* (Bacillariophyceae): A model study. *Harmful Algae* **2013**, *24*, 45–53. [[CrossRef](#)]
5. Trainer, V.L.; Hickey, B.M.; Horner, R.A. Biological and physical dynamics of domoic acid production off the Washington coast. *Limnol. Oceanogr.* **2002**, *47*, 1438–1446. [[CrossRef](#)]
6. Adams, N.G.; Lesoing, M.; Trainer, V.L. Environmental conditions associated with domoic acid in razor clams on the Washington coast. *J. Shellfish Res.* **2000**, *19*, 1007–1015.
7. Marchetti, A.; Trainer, V.L.; Harrison, P.J. Environmental conditions and phytoplankton dynamics associated with *Pseudo-nitzschia* abundance and domoic acid in the Juan de Fuca eddy. *Mar. Ecol. Prog. Ser.* **2004**, *281*, 1–12. [[CrossRef](#)]
8. Kudela, R.; Pitcher, G.; Probyn, T.; Figueiras, F.; Moita, T.; Trainer, V.L. Harmful algal blooms in coastal upwelling systems. *Oceanography* **2005**, *18*, 185–197. [[CrossRef](#)]
9. Anderson, C.R.; Brzezinski, M.A.; Washburn, L.; Kudela, R. Circulation and environmental conditions during a toxigenic *Pseudo-nitzschia australis* bloom in the Santa Barbara Channel, California. *Mar. Ecol. Prog. Ser.* **2006**, *327*, 119–133. [[CrossRef](#)]
10. Schnetzer, A.; Jones, B.H.; Schaffner, R.A.; Cetinic, I.; Fitzpatrick, E.; Miller, P.E.; Caron, D.A. Coastal upwelling linked to toxic *Pseudo-nitzschia australis* blooms in Los Angeles coastal waters, 2005–2007. *J. Plankton Res.* **2013**, *35*, 1080–1092. [[CrossRef](#)]
11. Figueiras, F.G.; Rios, A.F. Phytoplankton succession, red tides and the hydrographic regime in the Rías Bajas of Galicia. In *Toxic Phytoplankton Blooms in the Sea*; Smayda, T.J., Shimizu, Y., Eds.; Elsevier: Amsterdam, The Netherlands, 1993; pp. 239–244.
12. Moroño, A.; Pazos, Y.; Maneiro, J. Evolución del fitoplancton tóxico y condiciones oceanográficas asociadas en los años 97–98 en las Rías Gallegas. In Proceedings of the VI Reunión Ibérica sobre Fitoplancton Tóxico y Biotoxinas, Sevilla, Spain, 5–7 May 1999; Junta de Andalucía: Sevilla, Spain, 2000; pp. 59–66.
13. Palma, S.; Mouriño, H.; Silva, A.; Barao, M.; Moita, M.T. Can *Pseudo-nitzschia* blooms be modeled by coastal upwelling in Lisbon Bay? *Harmful Algae* **2010**, *9*, 294–303. [[CrossRef](#)]
14. González Vilas, L.; Spyarakos, E.; Torres Palenzuela, M.; Pazos, Y. Support Vector Machine-based method for predicting *Pseudo-nitzschia* spp. blooms in coastal waters (Galician rias, NW Spain). *Prog. Oceanogr.* **2014**, *124*, 66–77. [[CrossRef](#)]
15. Fawcett, A.; Pitcher, G.C.; Bernard, S.; Cembella, A.D.; Kudela, R.M. Contrasting wind patterns and toxigenic phytoplankton in the southern Benguela upwelling system. *Mar. Ecol. Prog. Ser.* **2007**, *348*, 19–31. [[CrossRef](#)]
16. Guannel, M.L.; Haring, D.; Twiner, M.J.; Wang, Z.; Noble, A.E.; Lee, P.A.; Saito, M.A.; Rocap, G. Toxigenicity and biogeography of the diatom *Pseudo-nitzschia* across distinct environmental regimes in the South Atlantic Ocean. *Mar. Ecol. Prog. Ser.* **2015**, *526*, 67–87. [[CrossRef](#)]

17. Louw, D.C.; Doucette, G.J.; Lundholm, N. Morphology and toxicity of *Pseudo-nitzschia* species in the northern Benguela Upwelling System. *Harmful Algae* **2018**, *75*, 118–128. [[CrossRef](#)] [[PubMed](#)]
18. Smith, J.C.; Cormier, R.; Worms, J.; Bird, C.J.; Quilliam, M.A.; Pocklington, R.; Angus, R.; Hanic, L. Toxic blooms of the domoic acid containing diatom *Nitzschia pungens* in the Cardigan River, Prince Edward Island. In *Toxic Marine Phytoplankton*; Graneli, E., Sundstrom, B., Edler, L., Anderson, D.M., Eds.; Elsevier: New York, NY, USA, 1990; pp. 227–232.
19. Parsons, M.L.; Dortch, Q.; Turner, R.E. Sedimentological evidence of an increase in *Pseudo-nitzschia* (Bacillariophyceae) abundance in response to coastal eutrophication. *Limnol. Oceanogr.* **2002**, *47*, 551–558. [[CrossRef](#)]
20. Kudela, R.; Cochlan, W.; Roberts, A. Spatial and temporal patterns of *Pseudo-nitzschia* species in central California related to regional oceanography. In *Harmful Algae 2002*; Steidinger, K.A., Landsberg, J.H., Tomas, C.R., Vargo, G.A., Eds.; Florida Fish and Wildlife Conservation Commission, Florida Institute of Oceanography, and Intergovernmental Oceanographic Commission of UNESCO: St. Petersburg, FL, USA, 2004; pp. 347–349.
21. GEOHAB. *Global Ecology and Oceanography of Harmful Algal Blooms, GEOHAB Core Research Project: HABs in Upwelling Systems*; Pitcher, P., Moita, T., Trainer, V.L., Kudela, R., Figueiras, P., Probyn, T., Eds.; IOC and SCOR.: Paris, France; Baltimore, MD, USA, 2005.
22. Klein, C.; Claquin, P.; Bouchart, V.; Le Roy, B.; Véron, B. Dynamics of *Pseudo-nitzschia* spp. and domoic acid production in a macrotidal ecosystem of the Eastern English Channel (Normandy, France). *Harmful Algae* **2010**, *9*, 218–226. [[CrossRef](#)]
23. Tas, S.; Lundholm, N. Temporal and spatial variability of the potentially toxic *Pseudo-nitzschia* spp. in a eutrophic estuary (Sea of Marmara). *J. Mar. Biol. Assoc. UK* **2017**, *97*, 1483–1494. [[CrossRef](#)]
24. Pednekar, S.M.; Bates, S.S.; Kerkar, V.; Prabhu Matondkar, S.G. Environmental Factors Affecting the Distribution of *Pseudo-nitzschia* in Two Monsoonal Estuaries of Western India and Effects of Salinity on Growth and Domoic Acid Production by *P. pungens*. *Estuaries Coasts* **2018**, *41*, 1448–1462. [[CrossRef](#)]
25. Horner, R.A.; Garrison, D.L.; Plumley, F.G. Harmful algal blooms and red tide problems on the US west coast. *Limnol. Oceanogr.* **1997**, *42*, 1076–1088. [[CrossRef](#)]
26. Trainer, V.L.; Pitcher, G.C.; Reguera, B.; Smayda, T.J. The distribution and impacts of harmful algal bloom species in eastern boundary upwelling systems. *Prog. Oceanogr.* **2010**, *85*, 33–52. [[CrossRef](#)]
27. Schnetzer, A.; Miller, O.; Schaffner, R.; Stauffer, B.; Jones, B.; Weisberg, S.; DiGiacomo, P.; Berelson, W.; Caron, D. Blooms of *Pseudo-nitzschia* and domoic acid in the San Pedro Channel and Los Angeles harbor areas of the Southern California Bight, 2003–2004. *Harmful Algae* **2007**, *6*, 372–387. [[CrossRef](#)]
28. Liefer, J.A.; Robertson, A.; MacIntyre, H.L.; Smith, W.L.; Dorsey, C.P. Characterization of a toxic *Pseudo-nitzschia* spp. bloom in the northern Gulf of Mexico associated with domoic acid accumulation in fish. *Harmful Algae* **2013**, *26*, 20–32. [[CrossRef](#)]
29. Bargu, S.; Baustian, M.M.; Rabalais, N.N.; Del Rio, R.; Von Korff, B.; Turner, R.E. Influence of the Mississippi River on *Pseudo-nitzschia* spp. Abundance and Toxicity in Louisiana Coastal Waters. *Estuaries Coasts* **2016**, *39*, 1345–1356. [[CrossRef](#)]
30. Pan, Y.; Subba Rao, D.V.; Mann, K.H. Changes in domoic acid production and cellular chemical composition of the toxigenic diatom *Pseudo-nitzschia multiseriata* under phosphate limitation. *J. Phycol.* **1996**, *32*, 371–381. [[CrossRef](#)]
31. Pan, Y.L.; Rao, D.V.S.; Mann, K.H.; Brown, R.G.; Pocklington, R. Effects of silicate limitation on production of domoic acid, a neurotoxin, by the diatom *Pseudo-nitzschia multiseriata*. 1. Batch culture studies. *Mar. Ecol. Prog. Ser.* **1996**, *131*, 225–233. [[CrossRef](#)]
32. Maldonado, M.T.; Hughes, M.P.; Rue, E.L.; Wells, M.C. The effect of Fe and Cu on growth and domoic acid production by *Pseudo-nitzschia multiseriata* and *Pseudo-nitzschia australis*. *Limnol. Oceanogr.* **2002**, *47*, 515–526. [[CrossRef](#)]
33. Fehling, J.; Davidson, K.; Bolch, C.J.; Bates, S.S. Growth and domoic acid production by *Pseudo-nitzschia seriata* (Bacillariophyceae) under phosphate and silicate limitation. *J. Phycol.* **2004**, *40*, 674–683. [[CrossRef](#)]
34. Wells, M.L.; Trick, C.G.; Cochlan, W.P.; Hughes, M.P.; Trainer, V.L. Domoic acid: The synergy of iron, copper, and the toxicity of diatoms. *Limnol. Oceanogr.* **2005**, *50*, 1908–1917. [[CrossRef](#)]
35. Auro, M.E.; Cochlan, W.P. Nitrogen Utilization and Toxin Production by Two Diatoms of the *Pseudo-nitzschia pseudodelicatissima* Complex: *P. cuspidata* and *P. fryxelliana*. *J. Phycol.* **2013**, *49*, 1529–8817. [[CrossRef](#)]

36. Trainer, V.L.; Bill, B.D.; Stehr, C.M.; Wekell, J.C.; Moeller, P.; Busman, M.; Woodruff, D. Domoic acid production near California coastal upwelling zones, June 1998. *Limnol. Oceanogr.* **2000**, *45*, 1818–1833. [[CrossRef](#)]
37. Trainer, V.L.; Hickey, B.M.; Lessard, E.J.; Cochlan, W.P.; Trick, C.G.; Wells, M.L.; MacFadyen, A.; Moore, S.K. Variability of *Pseudo-nitzschia* and domoic acid in the Juan de Fuca eddy region and its adjacent shelves. *Limnol. Oceanogr.* **2009**, *54*, 289–308. [[CrossRef](#)]
38. Downes-Tettmar, N.; Rowland, S.; Widdicombe, C.; Woodward, M.; Llewellyn, C. Seasonal variation in *Pseudo-nitzschia* spp. and domoic acid in the western English Channel. *Cont. Shelf Res.* **2013**, *53*, 40–49. [[CrossRef](#)]
39. Thorel, M.; Claquin, P.; Schapira, M.; Le Gendre, R.; Riou, P.; Goux, D.; Le Roy, B.; Raimbault, V.; Deton-Cabanillas, A.F.; Bazin, P.; et al. Nutrient ratios influence variability in *Pseudo-nitzschia* species diversity and particulate domoic acid production in the Bay of Seine (France). *Harmful Algae* **2017**, *68*, 192–205. [[CrossRef](#)] [[PubMed](#)]
40. Trick, C.G.; Trainer, V.L.; Cochlan, W.P.; Wells, M.L.; Beall, B.F. The successional formation and release of domoic acid in a *Pseudo-nitzschia* bloom in the Juan de Fuca Eddy: A drifter study. *Harmful Algae* **2018**, *79*, 105–114. [[CrossRef](#)] [[PubMed](#)]
41. Caroppo, C.; Congestri, R.; Bracchini, L.; Albertano, P. On the presence of *Pseudo-nitzschia calliantha* Lundholm, Moestrup et Hasle and *Pseudo-nitzschia delicatissima* (Cleve) Heiden in the Southern Adriatic Sea (Mediterranean Sea, Italy). *J. Plankton Res.* **2005**, *27*, 763–774. [[CrossRef](#)]
42. Zhu, Z.; Qu, P.; Fu, F.; Tennenbaum, N.; Tatters, A.O.; Hutchins, D.A. Understanding the blob bloom: Warming increases toxicity and abundance of the harmful bloom diatom *Pseudo-nitzschia* in California coastal waters. *Harmful Algae* **2017**, *67*, 36–43. [[CrossRef](#)] [[PubMed](#)]
43. Míguez, A.; Fernández, M.L.; Fraga, S. First detection of domoic acid in Galicia (NW Spain). In *Harmful and Toxic Algal Blooms*; Yasumoto, T., Oshima, Y., Fukuyo, Y., Eds.; Intergovernmental Commission of UNESCO: Paris, France, 1996; pp. 143–145.
44. Fraga, S.; Alvarez, M.J.; Míguez, A.; Fernández, M.L.; Costas, E.; Lopez-Rodas, V. *Pseudo-nitzschia* species isolated from Galician waters: Toxicity, DNA content and lectin binding assay. In *Harmful Algae*; Reguera, B., Blanco, B., Fernández, M.L., Wyatt, T., Eds.; Xunta de Galicia and Intergovernmental Commission of UNESCO: Santiago de Compostela, Spain, 1998; pp. 270–273.
45. Reguera, B.; Garcés, E.; Bravo, I.; Pazos, Y.; Ramilo, I.; González, G. Cell cycle patterns and estimates of in situ division rates of dinoflagellates of the genus *Dinophysis* by a postmitotic index. *Mar. Ecol. Prog. Ser.* **2003**, *249*, 117–131. [[CrossRef](#)]
46. Álvarez-Salgado, X.A.; Labarta, U.; Fernandez-Reiriz, M.J.; Figueiras, F.G.; Rosón, R.; Piedracoba, S.; Filgueira, R.; Cabanas, J.M. Renewal time and the impact of harmful algal blooms on the extensive mussel raft culture of the Iberian coastal upwelling system (SW Europe). *Harmful Algae* **2008**, *7*, 849–855. [[CrossRef](#)]
47. Rodríguez Rodríguez, G.; Villasante, S.; García-Negro, M. Are red tides affecting economically the commercialization of the Galician (NW Spain) mussel farming? *Mar. Policy* **2011**, *35*, 252–257. [[CrossRef](#)]
48. Arévalo, F.F.; Bermúdez, M.; Salgado, C. ASP toxicity in scallops: Individual variability and tissue distribution. In *Harmful Algae*; Reguera, B., Blanco, B., Fernández, M.L., Wyatt, T., Eds.; Xunta de Galicia and Intergovernmental Commission of UNESCO: Santiago de Compostela, Spain, 1998; pp. 499–502.
49. Garet, E.; González-Fernández, Á.; Lago, J.; Vieites, J.; Cabado, A. Comparative evaluation of Enzyme-linked Immunoassay and reference methods for the detection of shellfish hydrophilic toxins in several presentations of seafood. *J. Agric. Food Chem.* **2010**, *20*, 1410–1415. [[CrossRef](#)]
50. Maneiro, I.; Iglesias, P.; Guisande, C.; Riveiro, I.; Barreiro, A.; Zervoudaki, S.; Granéli, E. Fate of domoic acid ingested by the copepod *Acartia clausi*. *Mar. Biol.* **2005**, *148*, 123–130. [[CrossRef](#)]
51. Kudela, R.M.; Stumpf, R.P.; Petrov, P. Acquisition and analysis of remote sensing imagery of harmful algal blooms. In *Harmful Algal Blooms (HABs) and Desalination: A Guide to Impacts, Monitoring and Management*; Anderson, D.M., Boerlage, S.F.E., Dixon, M.B., Eds.; Intergovernmental Oceanographic Commission of UNESCO: Paris, France, 2017; pp. 119–132.
52. Zheng, G.; DiGiacomo, P.M. Uncertainties and applications of satellite-derived coastal water quality products. *Prog. Oceanogr.* **2017**, *159*, 45–72. [[CrossRef](#)]

53. Spyrakos, E.; González Vilas, L.; Torres Palenzuela, J.M.; Barton, E.D. Remote sensing chlorophyll a of optically complex waters (rias Baixas, NW Spain): Application of a regionally specific chlorophyll a algorithm for MERIS full resolution data during an upwelling cycle. *Remote Sens. Environ.* **2011**, *115*, 2471–2485. [[CrossRef](#)]
54. Doerffer, R.; Sorensen, K.; Aiken, J. MERIS potential for coastal zone applications. *Int. J. Remote Sens.* **1999**, *20*, 1809–1818. [[CrossRef](#)]
55. Donlon, C.; Berruti, B.; Buongiorno, A.; Ferreira, M.H.; Féménias, P.; Frerick, J.; Goryl, P.; Klein, U.; Laur, H.; Mavrocordatos, C.; et al. The Global Monitoring for Environment and Security (GMES) Sentinel-3 mission. *Remote Sens. Environ.* **2012**, *120*, 37–57. [[CrossRef](#)]
56. Barton, E.D.; Largier, J.L.; Torres, R.; Sheridan, M.; Trasviña, A.; Souza, A.; Pazos, Y.; Valle-Levinson, A. Coastal upwelling and downwelling forcing of circulation in a semi-enclosed bay: Ria de Vigo. *Prog. Oceanogr.* **2015**, *134*, 173–189. [[CrossRef](#)]
57. Pitcher, G.C.; Figueiras, F.G.; Hickey, B.M.; Moita, M.T. The physical oceanography of upwelling systems and the development of harmful algal blooms. *Prog. Oceanogr.* **2010**, *85*, 5–32. [[CrossRef](#)] [[PubMed](#)]
58. Zapata, M.; Rodríguez, F.; Garrido, J.L. Separation of chlorophylls and carotenoids from marine phytoplankton: A new HPLC method using a reversed phase C8 column and pyridine-containing mobile phases. *Mar. Ecol. Prog. Ser.* **2000**, *195*, 29–45. [[CrossRef](#)]
59. Strickland, J.; Parsons, T. *A Practical Handbook of Seawater Analysis*, 2nd ed.; Fisheries Research Board of Canada Bulletin: Ottawa, ON, Canada, 1972.
60. Van der Linde, D. *Protocol for Total Suspended Matter Estimate*; Technical Note No.I.98.182; European Commission, Joint Research Centre: Ispra, Italy, 1998.
61. Bendschneider, K.; Robinson, R. A new spectrophotometric method for the determination of nitrite in sea water. *J. Mar. Res.* **1952**, *11*, 87–96.
62. Wood, E.D.; Armstrong, F.A.J.; Richards, F.A. Determination of nitrate in seawater by cadmium copper reduction to nitrite. *J. Mar. Biol. Assoc. UK* **1967**, *47*, 23–31. [[CrossRef](#)]
63. Grasshoff, K.; Kremling, K.; Ehrhardt, K. *Methods of Seawater Analysis*, 3rd ed.; Wiley-VCH: New York, NY, USA, 1999.
64. Grasshoff, K.; Ehrhardt, M.; Kremling, K. *Methods of Seawater Analysis*, 2nd ed.; Verlag Chemie: Weinheim, FL, USA, 1983.
65. Utermöhl, H. Zur vervollkommnung der quantitativen phytoplankton-methodik. *Mitt. Int. Ver. Theor. Angewandte Limnol.* **1958**, *9*, 1–38. [[CrossRef](#)]
66. Tomas, C.R. *Identifying Marine Phytoplankton*; Academic Press: San Diego, CA, USA, 1997.
67. Renberg, I. A procedure for preparing large sets of diatom slides from sediment cores. *J. Paleolimnol.* **1990**, *4*, 87–90. [[CrossRef](#)]
68. Hasle, G.R.; Syvertsen, E.E. Marine diatoms. In *Identifying Marine Diatoms and Dinoflagellates*; Tomas, C.R., Ed.; Academic Press: San Diego, CA, USA, 1996; pp. 5–385.
69. Skov, J.; Lundholm, N.; Moestrup, Ø.; Larsen, J. Leaflet no. 185: Potentially toxic phytoplankton. The diatom genus *Pseudo-nitzschia* (Diatomophyceae/Bacillariophyceae). In *ICES Identification Leaflets for Phytoplankton*; Lindley, J.A., Ed.; ICES: Copenhagen, Denmark, 1999; pp. 1–23.
70. Fryxell, G.A.; Hasle, G.R. Taxonomy of harmful diatoms. In *Manual on Harmful Marine Microalgae, Monographs on Oceanographic Methodology*; Hallegraeff, G.M., Anderson, D.M., Cembella, A.D., Eds.; UNESCO: Paris, France, 2003; Volume 11, pp. 465–510.
71. Herrera, J.L.; Piedracoba, S.; Varela, R.A.; Roson, G. Spatial analysis of the wind field on the western coast of Galicia (NW Spain) from *in situ* measurements. *Cont. Shelf Res.* **2005**, *25*, 1728–1748. [[CrossRef](#)]
72. Bakun, A. *Coastal Upwelling Indices, West Coast of North America 1946–71*; Technical Report NMFS-SSRF 671; NOAA: Seattle, WA, USA, 1973; pp. 1–103.
73. Hidy, G.M. A view of recent air–Sea interaction research. *Bull. Am. Meteorol. Soc.* **1972**, *53*, 1083–1102. [[CrossRef](#)]
74. Beam 5, Brockmann Consult and Contributors. Available online: <http://www.brockmann-consult.de/cms/web/beam/> (accessed on 18 September 2019).
75. Doerffer, R.; Schiller, H. *MERIS Regional Coastal and Lake Case 2 Water Project—Atmospheric Correction ATBD*; GKSS Research Center: Geestacht, Germany, 2008; Version 1.0.

76. González Vilas, L.; Spyrakos, E.; Torres Palenzuela, J.M. Neural network estimation of chlorophyll a from MERIS full resolution data for the coastal waters of Galician rias (NW Spain). *Remote Sens. Environ.* **2011**, *115*, 524–535. [[CrossRef](#)]
77. Wood, S.N. Modelling and smoothing parameter estimation with multiple quadratic penalties. *J. R. Stat. Soc.* **2000**, *62*, 413–428. [[CrossRef](#)]
78. Lin, X.; Zhang, D. Inference in generalized additive mixed models using smoothing splines. *J. R. Stat. Soc.* **1999**, *61*, 381–400. [[CrossRef](#)]
79. Zuur, A.; Ieno, E.N.; Walker, N.; Saveliev, A.A.; Smith, G.M. *Mixed Effects Models and Extensions in Ecology With R*; Springer: New York, NY, USA, 2009.
80. Zuur, A.; Ieno, E.; Smith, G.M. *Analysing Ecological Data*; Springer: New York, NY, USA, 2007.
81. Prego, R.; Guzmán-Zuñiga, D.; Varela, M.; deCastro, M. Consequences of winter upwelling events on biogeochemical and phytoplankton patterns in a western Galician ria (NW Iberian peninsula). *Estuar. Coast. Shelf Sci.* **2007**, *73*, 409–422. [[CrossRef](#)]
82. Busse, L.; Venrick, E.; Antrobus, R.; Miller, P.; Vigilant, V.; Silver, M.; Mengelt, C.; Mydlarz, L.; Prezelin, B. Domoic acid in phytoplankton and fish in San Diego, CA, USA. *Harmful Algae* **2006**, *5*, 91–101. [[CrossRef](#)]
83. Garcia-Mendoza, E.; Rivas, D.; Olivos-Ortiz, A.; Almazan-Becerril, A.; Castaneda-Vega, C.; Pena-Manjarrez, J.L. A toxic *Pseudo-nitzschia* bloom in Todos Santos Bay, northwestern Baja California, Mexico. *Harmful Algae* **2009**, *8*, 493–503. [[CrossRef](#)]
84. Sekula-Wood, E.; Benitez-Nelson, C.; Morton, S.; Anderson, C.; Burrell, C.; Thunell, R. *Pseudo-nitzschia* and domoic acid fluxes in Santa Barbara Basin (CA) from 1993 to 2008. *Harmful Algae* **2011**, *10*, 567–575. [[CrossRef](#)]
85. Scholin, C.; Gulland, F.; Doucette, G.; Benson, S.; Busman, M.; Chavez, F.; Cordaro, J.; Delong, E.; Vogelaere, A.; Harvey, J.; et al. Mortality of sea lions along the central California coast linked to a toxic diatom bloom. *Nature* **2000**, *403*, 80–84. [[CrossRef](#)] [[PubMed](#)]
86. Parsons, M.L.; Dortch, Q.; Doucette, G. An assessment of *Pseudo-nitzschia* population dynamics and domoic acid production in coastal Louisiana. *Harmful Algae* **2013**, *30*, 65–77. [[CrossRef](#)]
87. Pazos, Y.; Moroño, A. Monitorización de condiciones oceanográficas y fitoplancton en las zonas de producción de moluscos de Galicia (2007–2010). In Proceedings of the XI Reunion Iberica, Fitoplancton Tóxico y Biotoxinas, Bilbao, Spain, 30 May–2 June 2011.
88. ICES. *Report of the ICES-IOC Working Group on Harmful Algal Bloom Dynamics (WGHABD)*; ICES CM 2008/OCC: Galway, Ireland, 2008.
89. ICES. *Report of the ICES—IOC Working Group on Harmful Algal Bloom Dynamics (WGHABD)*; ICES CM 2012/SSGHIE: Oban, UK, 2012.
90. Blanco, J.; De La Puente, M.B.; Arevalo, F.; Salgado, C.; Morono, A. Depuration of mussels (*Mytilus galloprovincialis*) contaminated with domoic acid. *Aquat. Living Resour.* **2002**, *15*, 53–60. [[CrossRef](#)]
91. Mafra, L.L., Jr.; Bricelj, V.M.; Fennel, K. Domoic acid uptake and elimination kinetics in oysters and mussels in relation to body size and anatomical distribution of toxin. *Aquat Toxicol.* **2010**, *100*, 17–29. [[CrossRef](#)] [[PubMed](#)]
92. Kvitck, R.G.; Goldberg, J.D.; Smith, G.J.; Doucette, G.J.; Silver, M.W. Domoic acid contamination within eight representative species from the benthic food web of Monterey Bay, California, USA. *Mar. Ecol. Prog. Ser.* **2008**, *367*, 35–47. [[CrossRef](#)]
93. Del Rio, R.; Bargu, S.; Baltz, D.; Fire, S.; Peterson, G.; Wang, Z. Gulf menhaden (*Brevoortia patronus*): A potential vector of domoic acid in coastal Louisiana food webs. *Harmful Algae* **2010**, *10*, 19–29. [[CrossRef](#)]
94. Blanco, J.; Acosta, C.P.; de la Puente, M.B.; Salgado, C. Depuration and anatomical distribution of the amnesic shellfish poisoning (ASP) toxin domoic acid in the king scallop *Pecten maximus*. *Aquat Toxicol.* **2002**, *60*, 111–121. [[CrossRef](#)]
95. Mauriz, A.; Blanco, J. Distribution and linkage of domoic acid (amnesic shellfish poisoning toxins) in subcellular fractions of the digestive gland of the scallop *Pecten maximus*. *Toxicon* **2010**, *55*, 606–611. [[CrossRef](#)]
96. Diaz, P.A.; Ruiz Villarreal, M.; Velo-Suarez, L.; Ramilo, I.; Gentien, P.; Lunven, M.; Fernand, L.; Raine, R.; Reguera, B. Tidal and wind-event variability and the distribution of two groups of *Pseudo-nitzschia* species in an upwelling-influenced ría. *Deep Sea Res. Part II Top. Stud. Oceanogr.* **2014**, *101*, 163–179. [[CrossRef](#)]

97. Silver, M.; Bargu, S.; Coale, S.; Benitez-Nelson, C.; Garcia, A.; Roberts, K.; Sekula-Wood, E.; Bruland, K.; Coale, K. Toxic diatoms and domoic acid in natural and iron enriched waters of the oceanic Pacific. *Proc. Natl. Acad. Sci. USA* **2010**, *107*, 20762–20767. [[CrossRef](#)] [[PubMed](#)]
98. Kleivdal, H.; Kristiansen, S.I.; Nilsen, M.V.; Briggs, L. Single-laboratory validation of Biosense Direct Competitive Enzyme-linked Immunosorbent Assay (ELISA) for the determination of Domoic acid toxins in shellfish. *J. AOAC Int.* **2007**, *90*, 1000–1010. [[PubMed](#)]
99. Lane, J.; Raimondi, P.; Kudela, R. Development of a logistic regression model for prediction of toxigenic *Pseudo-nitzschia* blooms in Monterey Bay, California. *Mar. Ecol. Prog. Ser.* **2009**, *383*, 37–51. [[CrossRef](#)]
100. Torres Palenzuela, J.; González Vilas, L.; Spyarakos, E. Artificial Neural Network model for predicting *Pseudo-nitzschia* spp. abundance in the Galician Rias (NW Spain). In Proceedings of the 14th International Conference on Harmful Algae, Crete, Greece, 1–5 November 2010.
101. Moroño, A.; Pazos, Y. Floraciones algales nocivas y condiciones oceanográficas en las rias gallegas durante los años 2007 y 2008. In Proceedings of the X Reunion Iberica, Fitoplancon Tóxico y Biotoxinas, Lisbon, Portugal, 12–15 May 2009.
102. Bates, S.S.; Defreitas, A.S.W.; Milley, J.E.; Pocklington, R.; Quilliam, M.A.; Smith, J.C.; Worms, J. Controls on domoic acid production by the diatom *Nitzschia-pungens* f. *multiseries* in culture—Nutrients and irradiance. *Can. J. Fish. Aquat. Sci.* **1991**, *48*, 1136–1144. [[CrossRef](#)]
103. Fehling, J.; Davidson, K.; Bates, S.S. Growth dynamics of non-toxic *Pseudonitzschia delicatissima* and toxic *P. seriata* (Bacillariophyceae) under simulated spring and summer photoperiods. *Harmful Algae* **2005**, *4*, 763–769. [[CrossRef](#)]
104. Fehling, J.; Davidson, K.; Bolch, C.J.; Tett, P. Seasonality of *Pseudo-nitzschia* spp. (Bacillariophyceae) in western Scottish waters. *Mar. Ecol. Prog. Ser.* **2006**, *323*, 91–105. [[CrossRef](#)]
105. Davidson, K.; Gowen, R.; Tett, P.; Bresnan, E.; Harrison, P.; McKinney, A.; Milligan, S.; Mills, D.; Silke, J.; Crooks, A.M. Harmful algal blooms: How strong is the evidence that nutrient ratios and forms influence their occurrence? *Estuar. Coast. Shelf Sci.* **2012**, *115*, 399–413. [[CrossRef](#)]
106. Thessen, A.E.; Stoecker, D.K. Distribution, abundance and domoic acid analysis of the toxic diatom genus *Pseudo-nitzschia* from the Chesapeake Bay. *Estuaries Coasts* **2008**, *31*, 664–672. [[CrossRef](#)]
107. Lefebvre, K.A.; Robertson, A. Domoic acid and human exposure risks: A review. *Toxicon* **2010**, *56*, 218–230. [[CrossRef](#)]
108. Anderson, C.R.; Siegel, D.A.; Kudela, R.M.; Brzezinski, M.A. Empirical models of toxigenic *Pseudo-nitzschia* blooms: Potential use as a remote detection tool in the Santa Barbara Channel. *Harmful Algae* **2009**, *8*, 478–492. [[CrossRef](#)]
109. CoastObs Project. Available online: <http://coastobs.eu/> (accessed on 18 September 2019).



© 2019 by the authors. Licensee MDPI, Basel, Switzerland. This article is an open access article distributed under the terms and conditions of the Creative Commons Attribution (CC BY) license (<http://creativecommons.org/licenses/by/4.0/>).